Quantitative Paleoflood Hydrology☆

Gerardo Benito[a], Tessa M Harden[b], and Jim O'Connor[c], [a]Spanish National Research Council (CSIC), National Museum of Natural Sciences (MNCN), Madrid, Spain; [b]Oregon Water Science Center, U.S. Geological Survey, Portland, OR, United States; [c]U.S. Geological Survey, Portland, OR, United States

1 Introduction

Paleoflood hydrology Kochel and Baker (1982) is the reconstruction of the magnitude and frequency of past floods using geological evidence (Baker et al., 2002). Over the last 40 years, paleoflood hydrology has achieved recognition as a new branch of geomorphology and hydrology (Baker, 2008; Benito and Thorndycraft, 2005; Wilhelm et al., 2019), employing principles of geology, biology, hydrology, and fluid dynamics to infer quantitative and qualitative aspects of unobserved or unmeasured floods on the basis of physical evidence left in their wake (House et al., 2002). Flood indicators include various types of geologic evidence (flood deposits and geomorphic features) and flotsam deposits, as well as physical effects on vegetation. Resulting inferences can include timing, magnitude, and frequency of individual floods at specific sites or for specific rivers, as well as conclusions regarding the magnitude and frequency of channel forming floods. The obvious benefit of paleoflood studies is obtaining information on floods from periods of time or locations lacking direct measurements and observations thereby extending the systematic record especially with regards to large floods. Paleoflood studies have been used to support flood hazard assessments as well as understanding of the linkages between climate, land-use, flood frequency and channel morphology.

The primary goal of paleoflood hydrology is to acquire information on extreme floods by inferring their hydrological parameters (usually flood discharge) from physical evidence, thereby contrasting with standard flood hydrology based on direct measurements of hydrologic phenomena. Paleoflood studies involve many different techniques, the selection of which is mainly guided by (1) attributes of the river system; and (2) the purpose of the flood study. The physical characteristics of a river system dictate the type, longevity, and fidelity of paleoflood records. The purpose of a flood study gives priority to relevant evidence and analyses of paleostage indicators, its age (numerical or relative), and hydraulic properties.

Paleoflood studies typically take one of two forms: (1) analyses focused on determining quantitative information for specific events, such as the timing, peak discharge, and maximum stage of an individual flood or floods; and (2) studies investigating more general spatial and temporal patterns of flooding, commonly to assess relations among climate, land-use, flood frequency and magnitude, and geomorphic response (such as channel morphology or floodplain sedimentation and erosion processes). Both types of investigations share approaches and techniques, but, in general, studies to determine the quantitative information for specific events are most typically conducted in bedrock or otherwise confined river systems for which preservation of stratigraphic and geomorphic records of individual floods are more likely (Kochel and Baker, 1982). In the last decade, new approaches and paleoflood archives emerged to construct on-site and regional flood datasets derived from lake sediments (e.g., Amann et al., 2015; Corella et al., 2016; Kämpf et al., 2019; Munoz et al., 2018; Schillereff et al., 2016; Wilhelm et al., 2012, 2016; Wirth et al., 2013), speleothems (e.g., Denniston and Luetscher, 2017; Feinberg et al., 2019; Gonzalez-Lemos et al., 2015), and alluvial river environments (e.g., Jones et al., 2012; Knox and Daniels, 2002; Macklin et al., 2015; Munoz et al., 2018; Schulte et al., 2015; Toonen et al., 2015; Wang and Leigh, 2012). Recent reviews of those various flood archives and methods involved were provided by Benito and Díez-Herrero (2015), Wilhelm et al. (2018), Wilhelm et al. (2019), and Schulte et al. (2019).

☆*Change History*: March 2020. G Benito et al. updated text, added new figures, i.e., Figs. 1, 5, and 6, and Table 1. Modified Figs. 2, 3, and 4. A new author, Tessa Harden, was also involved.

This article focuses on techniques and approaches for obtaining quantitative information on specific floods in fluvial systems—as this has been the main emphasis of most paleoflood studies of the last 40 years—and provides example applications for different scientific and engineering problems.

2 Quantitative paleoflood hydrology

Quantitative paleoflood hydrology relies on identification of evidence of flooding in conjunction with application of hydrodynamic principles to determine flow magnitude. These two aspects of investigation typically lead to four components of analysis: (1) documentation and assessment of flood evidence; (2) determination of paleoflood ages; (3) estimation of flow magnitude, typically peak discharge associated with flood evidence; and (4) incorporation of paleoflood data into the flood frequency analysis. The first component is geological and archival, requiring classic tools of historical research, geomorphology, stratigraphy, and sedimentology. The second component involves geochronology in order to identify and date physical evidence of flooding. The third component requires hydraulic and hydrodynamic analyses, typically drawn from engineering applications, to assign a flow magnitude to paleoflood evidence. The fourth component combines paleoflood discharge data with instrumental streamflow records into flood frequency analyses to more accurately estimate flood quantiles at low annual exceedance probabilities. These paleoflood studies generally are more successful and have fewer uncertainties in fluvial systems with resistant boundaries, such as bedrock or semi-alluvial channels. These relatively stable types of river systems typically better preserve stratigraphic records from floods; some records exceed several thousand years. Additionally, the assumption of the present channel geometry being appropriate for estimating past hydraulic conditions is more reliable for bedrock or stable-boundary channels than it is for alluvial rivers.

Paleoflood studies in bedrock rivers gained traction in the late 1970s and early 1980s, primarily under the auspices of Prof. Victor R. Baker and his students in the southwestern United States. Over the last 40 years, the approach has gained worldwide application (Table. 1). Most of these paleoflood studies in bedrock rivers were carried out in semiarid and arid regions (Fig. 1).

Table 1 Quantitative paleoflood hydrology studies based on evidence from slackwater flood deposits (SWD).

World region	*Country*	*State/river*	*References*
North America	United States	Texas	Kochel et al. (1982)
		Arizona	Ely and Baker (1985); Ely et al. (1993); House et al. (2002); O'Connor et al. (1994); Partridge and Baker (1987)
		Utah and Colorado	Greenbaum et al. (2014a); Liu et al. (2019); O'Connor et al. (1986); Webb et al. (2002); Jarrett (1990)
		Wisconsin	Knox (1985)
		S. California	Enzel (1992)
		Washington, Oregon and Idaho	Chatters and Hoover (1986); Chatters and Hoover (1992); Hosman and Ely (2003); Beebee and O'Connor (2013)
		South Dakota	Harden et al. (2011)
South America	Peru	Central	Magilligan et al. (2008); Wells (1990)
	Chile	Atacama	Miller et al. (2019)
		Patagonia	Benito and Thorndycraft (2020); Benito et al. (2014); Dussaillant et al. (2010)
Australia	Australia	Central and Eastern parts	Erskine and Peacock (2002); Lam et al. (2017a); Lam et al. (2017c); Patton et al. (1993); Sandercock and Wyrwoll (2005); Wohl (1992); Wohl et al. (1994)
Europe	Spain	Tagus R., Llobregat R. Guadiana R., Segura R., Guadalquivir R., R. Viuda	Benito et al. (2003c, 2010, 2020); Bohorquez et al. (2013); Garcia-Garcia et al. (2013); Garrote et al. (2018); Machado et al. (2017); Ortega and Garzón (2009); Ruiz-Villanueva et al. (2013); Ruiz-Villanueva et al. (2010); Thorndycraft et al. (2005a)
	France	Ardeche R., Gardon R.	Dezileau et al. (2014); Sheffer et al. (2003); Sheffer et al. (2008)
	Greece	Crete	Macklin et al. (2010)
Middle East	Israel	Nahal Zin, Negev Desert	Greenbaum et al. (2006); Greenbaum et al. (2000); Greenbaum et al. (2020)
South Asia	India	Narmada and Tapi rivers	Ely et al. (1996); Kale et al. (1997); Kale et al. (2003)
		Lower Ganga	Goodbred and Kuehl (2000)
		Kaveri river	Goswami et al. (2019); Kale et al. (2010)
		Mahi R.; Sabarmati R.	Sridhar (2007); Sridhar et al. (2014)
	Thailand	Northern Thailand	Kidson et al. (2006)
Northern Asia	South Korea	Yugu, Pyeongchang and Dong rivers	Kim and Tanaka (2017); Lim et al. (2013)
	China	Yangtze R.	Guo et al. (2016); Wang et al. (2011); Zhan et al. (2010); Zhu et al. (2005)
		HanShui (Hanjiang) River	Huang et al. (2013); Liu et al. (2015); Mao et al. (2016)
		Yellow R.	Fan et al. (2015); Hu et al. (2016); Li and Huang (2017); Liu et al. (2014); Yang et al. (2000)
		Weihe, Qishuihe, Yanhe rivers	Huang et al. (2012); Wan et al. (2019); Zhang et al. (2012), Huang et al. (2011) Guo et al. (2017)
Africa	South Africa	Umgeni R., Orange R., Buffels R.	Benito et al. (2011a); Benito et al. (2011b); Smith (1992); Zawada (1994); Zawada (2000)
	Namibia	Namib desert; Kuiseb R., Fish R.	Cloete et al. (2018); Greenbaum et al. (2014b); Grodek et al. (2013); Heine (2004); Heine and Völkel (2011)

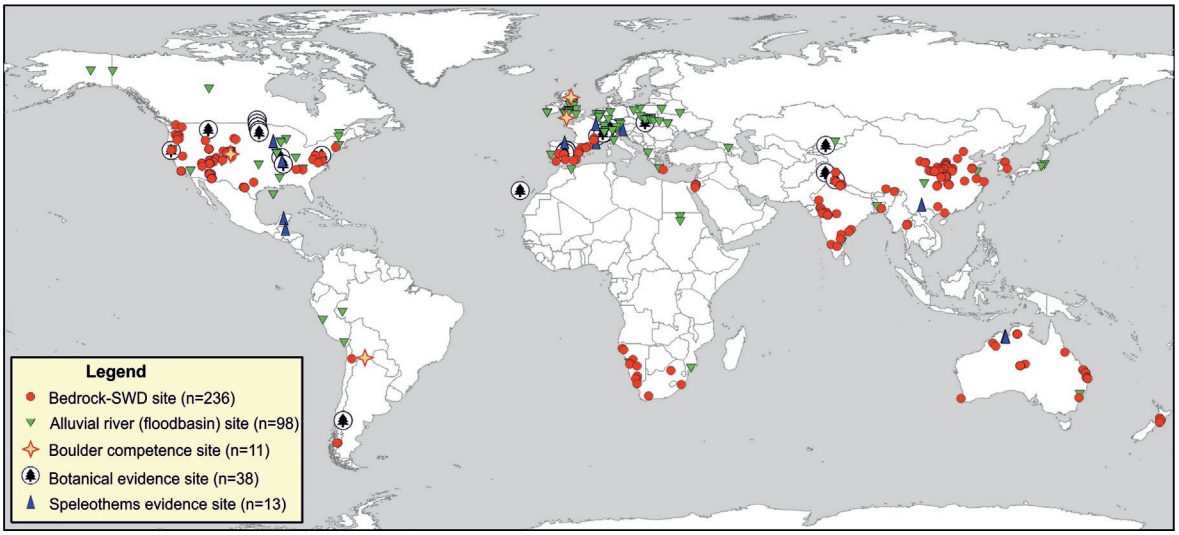

Fig. 1 World distribution of the most representative paleoflood studies in rivers. Paleoflood data sites from PAGES Floods Working Group.

Beyond narrow bedrock canyons and dryland regions, quantitative paleoflood hydrology has been applied on expansion-constriction and backwater settings of Australian macrochannels (Lam et al., 2017a,b), and in expansion reaches of semiconfined rivers of India (Kale et al., 2010; Wasson et al., 2013) and China (Huang et al., 2013; Zhang et al., 2012). More recently, studies on the Tennessee River in the southeastern United States have shown promise for expanding the approach to more humid environments (Harden and O'Connor, 2017; Davis et al., 2019). Humid regions have typically been avoided due to the increased potential for bioturbation from vegetation, insects, and animals as well as the potential to preserve organic material used for radiocarbon analysis. Some aspects of these techniques have also been also applied to water flows related to megafloods and catastrophic floods in Earth and Mars (e.g., Baker, 2020; Benito and Thorndycraft, 2020; O'Connor et al., 2013). In general, paleoflood studies show that (1) flood discharges estimated for paleofloods have commonly exceeded those of the observed record (Enzel et al., 1993); and (2), in certain areas, very large floods cluster on time scales of decades and centuries, interpreted as a flood response to climate variability (Benito et al., 2015a,b; Ely et al., 1993; Harden et al., 2010, 2015; Knox, 2000).

2.1 Flood geomorphology

Paleoflood records can be reconstructed from two basic types of physical evidence: High-water marks, and paleostage indicators. High water marks include mud, silt, seed lines and flotsam (e.g., fine organic debris, grass, woody debris) that closely mark peak flood stage (Koenig et al., 2016). This type of evidence typically only persists for weeks, in humid climates, to several years, in semiarid and arid climates (Williams and Costa, 1988). In contrast, paleostage indicators provide longer lasting evidence of peak flow stages, and typically consist of fine-textured flood sediment (slack-water flood deposits; e.g., Fig. 2C), gravel and boulder bars, silt lines, and erosion features (Herget, 2020; Kochel and Baker, 1988; Koenig et al., 2016), as well as durable botanical evidence such as scars on riparian trees (McCord, 1996). Depending on the environment, such evidence can persist for several millennia (Kochel and Baker, 1982).

Silt lines are subhorizontal linear deposits of silt- and clay-sized particles preserved on bedrock canyon walls, providing clear evidence of maximum flood stage (Fig. 2A). These lines have been interpreted as derived from suspended load of the flooded stream, being left as the flood waters covered and, in places, percolated into the bedrock valley margins (O'Connor et al., 1986). Such silt lines are uncommon and require distinction from other processes leaving such marks on canyon walls, such as may result from erosion of former gravel or sand patches.

High level scour marks and trimlines on valley-margin colluvium and soils may result from erosion of largest(s) floods (Fig. 2B), although their interpretation may be ambiguous (Webb and Jarrett, 2002). In high gradient streams, coarse boulder deposits are the most common large-flood deposits and can also serve as paleostage indicators (Jarrett, 1990).

Botanical flood evidence include flood scars and other flood-related effects on riparian trees (sprouting from tilting steams, eccentric ring growth (Sigafoos, 1964), which have been used effectively for reconstructing regional flood magnitude and frequency (Ballesteros-Cánovas et al., 2015a; St George, 2010). A tree-ring paleoflood study typically involves (1) identification of flood-affected trees at the specific reach, (2) sampling by core (increment borer) or by slab of stems, branches or roots, as close as possible to evident flood damage, (3) identification of "flood rings" (St George and Nielsen, 2003) and compilation of flood chronology, and (4) spatial analysis of damage types and intensity during single events (spatial connectivity and Wit index; (Schneuwly-Bollschweiler et al., 2013). Recently, Ballesteros-Cánovas et al. (2015b) described new techniques to infer flood history from

Fig. 2 Field examples of paleoflood stage indicators. (A) Silt lines preserved on canyon walls, Buckskin Gulch (Utah). (B) Flood trimline on coarse colluvium deposits, upper Fish River catchment (Namibia) (Cloete et al., 2018). (C) Sequence of 144 beds of Holocene slackwater flood deposits in the Nef valley, about 2 km from the Baker-Nef confluence in the Chilean Patagonia (Benito and Thorndycraft, 2020). (D) Flood benches, at 17 and 10 m above the present channel bottom, deposited in a valley expansion within the Tagus River gorge (Central Spain; Benito et al., 2003c). (E) Flood bench at a backwater flooded tributary of the Kuiseb River (Namibia; Grodek et al., 2013). (F) Rock shelter partly filled with slackwater flood deposits flanking Rapid Creek (western South Dakota; Harden et al., 2011). *SWD*, slackwater flood deposits.

tree-ring anatomical changes, even in the absence of physical external evidence of flood damage (St George et al., 2002). For example, prolonged anoxic conditions in the root system can influence the production and transport of growth hormones (e.g., auxin), inducing changes in wood anatomy (Wertz et al., 2013). These vessel-size anatomical changes have been used to identify and reconstruct summer floods in rivers with mixed flood populations (e.g., summer floods, Yanosky, 1984).

The longest paleoflood records generally result from analysis of paleostage indicators consisting of stratigraphic sequences of fine-grained flood deposits (Fig. 2C). Such deposits can accumulate for many millennia, recording large floods. Most paleoflood studies aiming to improve flood frequency analysis rely on such deposits. Such studies require locating appropriate sites, detailed

stratigraphic and geochronologic analysis, hydraulic studies to relate deposits to paleoflood discharges, and flood frequency analysis incorporating the paleoflood information.

Broad assessment of potential paleoflood sites can be obtained from desktop GIS analyses of topography and geology (e.g., O'Connor et al., 2014). Key elements are sources of fine grained sediment sources within the catchment area and conditions facilitating accumulation and preservation of stratigraphic records. Rivers within ideal fine sediment-producing geology (such as granite, diorite, and sandstone) are most likely to have high suspended sediment loads during floods. Some of the most ideal paleoflood sites are downstream of aeolian dunefields, including the paleo-aeolian sand and loess deposits of the Namib Desert (Cloete et al., 2018; Greenbaum et al., 2014b; Grodek et al., 2013), the Chinese Loess Plateau (Yellow River, e.g., Hu et al., 2016; Huang et al., 2013; Yang et al., 2000) and Tibetan Plateau (Yantzee River, e.g., Guo et al., 2016; Huang et al., 2013; Liu et al., 2015).

More specific site selection commonly requires field reconnaissance, typically after preliminary assessment of aerial imagery and topographic information. The search for sites is greatly assisted by tracing evidence of large historical floods, which commonly signal locations of evidence of prehistoric floods (e.g., Harden and O'Connor, 2017; Harden et al., 2011). The number and types of sites chosen for detailed stratigraphic and geochronologic analysis depends foremost on site availability and access, but also on the study objectives. For analyses striving to improve flood frequency estimates for rare, large magnitude floods using current statistical techniques, best results typically result from an ensemble of geologic evidence, including:

(1) Multiple sites of preserved flood stratigraphy so to evaluate consistency and completeness of the record among sites.
(2) Sites of preserved flood stratigraphy at different elevations so to differentiate the relative and absolute magnitude of floods recorded by the deposits. A flood only recorded at low-elevation deposits may be inferred to be smaller than those recorded at high elevation sites. Low elevation sites may record more floods and/or more recent floods; whereas higher sites may host longer records of very large floods (e.g., Benito et al., 2003a).
(3) In conjunction with (2), a distribution of sites, depositional records, and geochronology enabling identification of multiple flood perception or censoring thresholds and associated time intervals. For current flood frequency analysis techniques, such information frames the consideration of individual floods recorded by geologic or non-systematic historical evidence (e.g., Botero and Francés, 2010; England et al., 2019).
(4) In some situations, evidence of non-inundation, such as landforms or locations that can be inferred *not to have been flooded* for specific periods. Such non-exceedance bounds (Cloete et al., 2018; Levish, 2002), can constrain the right-hand tail of calculated flood frequency distributions (O'Connell et al., 2002).

Paleoflood depositional environments (Fig. 3) commonly include (1) areas of channel widening, (2) severe channel bends and valley expansion (Fig. 2D), (3) obstacle hydraulic shadows where flow separation causes eddies, (4) back-flooded tributary mouths and valleys (Figs. 2E), (5) alcoves and caves in bedrock walls (Fig. 2F), and (6) the tops of high alluvial or bedrock surfaces adjacent to the channel (e.g., Benito et al., 2003b, 2020; Harden and O'Connor, 2017; Harden et al., 2011; Kochel and Baker, 1988; Kochel et al., 1982; Li et al., 2019; Thorndycraft et al., 2005a; Zhang et al., 2013). The first three depositional environments owe to flow separation and recirculation zones downstream from flow perturbations. The flow pattern of recirculation zones consists of a

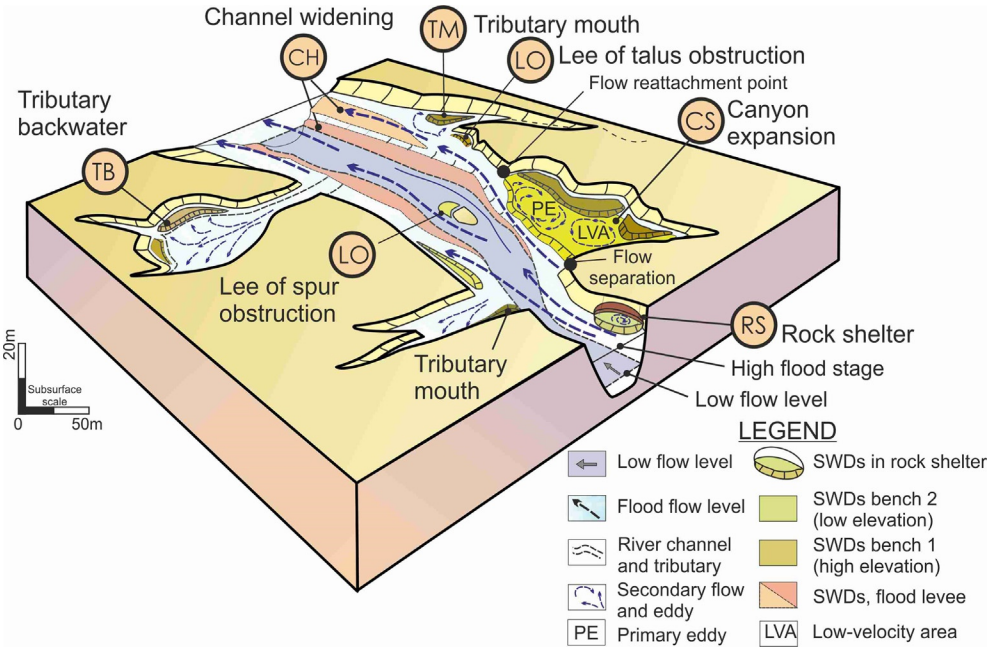

Fig. 3 Block diagram illustrating the location of sedimentary environments related to flood deposition. Modified from Benito G, Sanchez-Moya Y, Sopena A (2003b) Sedimentology of high-stage flood deposits of the Tagus River, Central Spain. *Sedimentary Geology* 157: 107–132.

primary eddy that fills at low discharge the central and downstream parts of the recirculation zone (side expansion), but at higher discharge one or more secondary eddies and areas of low velocity occurs upstream of the primary eddy (Rubin et al., 1990). This flow pattern causes deposition of suspended load in these valley-side expansion zones (Fig. 3), typically forming a reattachment bar located at the downstream end and beneath the primary eddy, and a separation bar located upstream (Schmidt, 1990). Discharge variation causes changes in the location of the reattachment and separation points, as well as the location of erosion and potential deposition sites. Paleoflood sedimentation is typically preserved at stagnation zones near the separation and reattachment points (Fig. 3). The resulting flood deposits commonly contain current-produced sedimentary structures, such as climbing ripples and cross-lamination, and a variety of textures owing to varying flow energy, direction and velocity within a recirculation cell during the course of the flood (Fig. 4B).

Caves, deep alcoves, back-flood tributary mouths, and distal overbanks are typically less energetic depositional environments (Fig. 2E and F). Such slackwater environments typically accumulate finer deposits, fine to very fine sand, silt and occasionally clay. These sites commonly host the longest and most complete records. Sedimentary structures are typically parallel lamination, massive structure and less commonly current ripples, reflecting slack flow energy conditions (Fig. 4C).

The character, completeness, and duration of the resulting stratigraphic record depends on the local depositional environment relative to flood hydraulics and the sediment load. The most complete and durable records are in quiet "slackwater" environments where the suspended load settles out without eroding previously emplaced deposits. Caves and alcoves, inundated, but away from the main channel, may shelter such deposits for millennia (e.g., Baker et al., 1983; Harden et al., 2011; O'Connor et al., 1994; Benito et al., 2020). More proximal deposits, adjacent to the channel but in flow separation zones, such as eddy bars, backflooded tributary mouths, and in the lee of valley obstructions, are typically coarser and commonly stratigraphically complex, affected by both flood

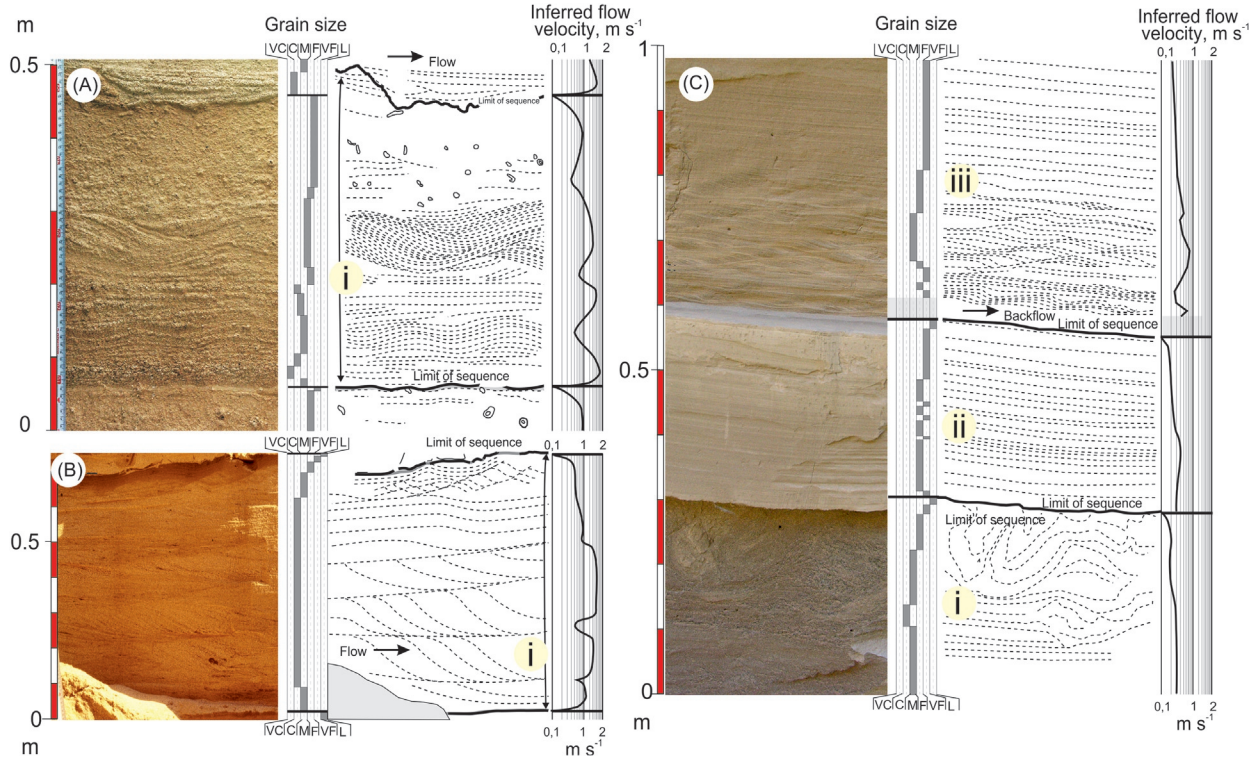

Fig. 4 Selected flood sequences and representative facies from slackwater flood deposits, interpretation of sedimentary structures, grain size and inferred flow velocity. (A) Photograph of sediment peel (described in the next section; 50 cm high) of slackwater flood deposits from the Guadalentín River (Spain, Benito et al., 2010). The sequence (i) shows, at the base, coarse to medium sand with parallel lamination and three dimensional bedforms that resemble hummocky cross-stratification. This fining upwards sequence culminates with parallel lamination and bioturbated sand that locally includes clay chips. This sedimentary sequence is inferred to have resulted from extreme floods with high stream flow velocity (>1 m s^{-1}) in a near-channel flow separation zone. (B) Field photograph of a flood sequence (flood i) in a channel widening area of the Tagus River (Spain, Benito et al., 2003a). The sequence is composed at the base by coarse to medium sand with planar cross-bedding overlain by climbing ripples and capped by silty clay with mud cracks. Note that the overlying flood sand unit contains mud rip-up clast and mud chips eroded from the upper laminae of the flood sequence. (C) Field photograph of slackwater flood deposits within a back-flooded tributary environment showing three flood units (Kuiseb River, Namibia, site K-400, Grodek et al., 2013). The lower sequence (flood i) contains parallel lamination deformed by fluid escape structures or convolute bedding due to density inversion. The intermediate sequence (flood ii) is composed of fine to very-fine sand with parallel lamination produced by aggradation on a plane bed and is capped by clayey silt. The upper sequence (flood iii) contains fine-grained sand with in-phase climbing ripples, overlain by very fine-grained sand with parallel lamination. The lower ripple structures show lamina dipping up the tributary valley deposited during the rising flood stage of the Kuiseb River. The upper sand with parallel lamination was deposited later during the same flood, but near the time of peak stage during flow stagnation in the backflooded tributary.

erosion and deposition (Benito et al., 2003c; Grodek et al., 2013; Zhang et al., 2012). Nevertheless, such sites can contain valuable records, particularly if the more energetic deposits more accurately mark maximum flood stages (Cloete et al., 2018; Greenbaum et al., 2020).

2.2 Stratigraphy and sedimentology

For flood chronology and frequency assessments, stratigraphic analysis emphasizes breaks and contacts separating individual flood deposits, and sedimentary textures and structures indicative of depositional process and sediment source (Fig. 4). Individual flood deposits within a stratigraphic profile can be identified by the following criteria (e.g., Benito et al., 2003b; Enzel et al., 1994; Kochel and Baker, 1988):

(1) Identification of a distinct silt to clay layer at the top of a flood unit, recording the waning stage of a flood;
(2) Intervening layers of sediments deposited by non-flood processes. These commonly include colluvium, cave roof-fall, and tributary alluvium that separate deposits of main-stem floods;
(3) Bioturbation (plant and animal activity) indicative of an exposed sedimentary surface;
(4) An erosional boundary where the surface of an older flood unit has been eroded by a later flood event;
(5) A change in the physical characteristics of the flood units, such as sediment color or particle size, that may be brought about by factors such as differing sediment source or differing energy conditions during separate flood events. This criterion is not always valid by itself and may need additional support by other indicators of subaerial exposure.
(6) Development of paleosols and associated pedogenic alterations to sedimentary units.

Sedimentary structures developed within individual flood units provide valuable information on the flow energy and sediment pulses during single flood events (Benito et al., 2003b; Kochel and Baker, 1988; McKee, 1938; e.g., Fig. 4C, unit iii). Within high-energy eddy zones, sedimentology typically consists of medium to coarse sand with high-energy parallel lamination, large-scale planar or trough cross-bedding, ripple lamination and massive intervals (Fig. 4A and B). Within more low-energy slack-water areas, textures are dominated by silty sand and sandy silt, with parallel lamination (Fig. 4C).

The stratigraphy at paleoflood sites may contain deposits of non-fluvial origin, such as aeolian sands or local slope deposits (Benito et al., 2003b). In temperate and subtropical climates, soils can rapidly form on paleoflood sediments depending on the time interval between flood events (Lam et al., 2017a). In China, paleoflood deposits are often intermixed with aeolian loess deposits (Huang et al., 2013; Zhou et al., 2016). In the Yangtze and Yellow river catchments, particle size distribution is used to differentiate SWDs featuring peaks of well sorted very fine sand (>63 μm), from eaolian loess made of coarse silt (16–63 μm) and fine silt (4–16 μm), and paleosol horizons with fine silt to clay (2–16 μm) (Huang et al., 2013; Mao et al., 2016; Zhang et al., 2012).

A complementary technique for sedimentological analysis consists of preparation of sediment peels of selected portions of the stratigraphic profile (Benito et al., 2003b; Hattingh and Zawada, 1996). Sediment peels are made by adhering sediments from a planar exposure of slack-water sediment outcrop onto fabric, preserving a coating of sediment and their sedimentary structures (Fig. 4A). This technique allows for a very detailed description and analysis of textural variations and sedimentary structures for individual flood units as well as improving interpretation of hydrodynamic changes such as flow velocity during flood events (Benito et al., 2010).

2.3 Non-exceedance bounds

Some recent paleoflood studies have focused on evidence for non-inundation bounds. A non-exceedance bound is defined as a time interval during which a paleostage has not been exceeded sufficiently to modify a terrace or abandoned floodplain surface (non-exceedance discharge threshold, (Levish, 2002)). Stable terraces have been used as the field expression of upper limits of flooding over a time interval established by geochronological means (England et al., 2010; Godaire and Bauer, 2013). But caution is needed in inferring the absence of floods from the absence of evidence. Although non-exceedance bounds are statistically powerful, application can be uncertain, particularly when applied to geologic and geomorphic situations because of the variety of mechanisms by which large floods may fail to leave a recognizable depositional or erosional trace on a landform. Non-exceedance bounds, if appropriately applied in a flood frequency analysis, can provide powerful constraints on the flood frequency distribution of extreme floods (see section 2.7).

2.4 Paleoflood records from Alluvial Rivers

Flood histories can also be derived from unconfined alluvial rivers. Unlike bedrock rivers with stable and confined boundaries, the dynamic nature of alluvial rivers can present challenges regarding deposit preservation and estimating discharges associated with paleoflood records. The common approaches include employing botanical evidence, especially tree-based chronologies of floods (e.g., Ballesteros-Cánovas et al., 2015b; St George, 2010), and, for longer records, investigation of alluvial stratigraphy preserved within floodplain deposits, particularly vertical and lateral accretionary units on floodplain surfaces, and within abandoned channels and oxbow lakes (Macklin et al., 2012; Toonen et al., 2012, 2020; Wang and Leigh, 2012). Some alluvial floodplain environments are excellent flood sediment sinks (Lewin et al., 2017) but differentiation and reconstruction of flood records can be

difficult due to low or varying depositional rates or channel migration. Detailed stratigraphic analysis of field exposures or from sediment cores allows for identification of individual flood deposits based on similar criteria for distinguishing flood layers in bedrock-canyon slackwater deposits (Knox, 1985). But investigators working on floodplain deposits, where contacts are commonly obscured by bioturbations and pedogenic processes, commonly use additional tools and measurements, such as magnetic susceptibility, geochemical or mineralogical composition, and grain-size changes to differentiate deposits (Knox and Daniels, 2002). Such techniques have gained traction in recent years during which a wide range of methods for geochemical and textural analysis from core samples have been used to identify individual flood events, and to infer changes on magnitude and frequency, commonly supported by robust age-depth models (e.g., Jones et al., 2012; Toonen et al., 2015).

For example, in the River Severn (United Kingdom), the relative flood magnitude of a c. 3750 year flood record was determined from changes in the inorganic element ratio of zirconium and rubidium (Zr/Rb), as a geochemical grain-size proxy correlated to flood discharge magnitudes at nearby gaging stations (Jones et al., 2012). Another recent example is the analysis of paleoflood records from abandoned channel fills and oxbow lakes in distal parts of the floodplain in delta environments of the river Rhine in the Dutch-German delta region (Toonen et al., 2012). Subaqueous environments in the floodplain (oxbow lakes and dike breach scour holes), often contain continuous records of clastic deposits separated by organic-rich layers. In certain alluvial environments, grain size variations within flood deposits may indicate flood magnitude (e.g., Toonen et al., 2020).

2.5 Paleoflood age determination

Dating of sedimentary flood units and intervening deposits is a key task supporting analysis of temporal flood behavior and recurrence. Dating methods applied in paleoflood hydrology can be divided into three categories (Jacobson et al., 2016): numerical, relative, and hybrid-correlated. Development of a time-scale sequence of paleofloods requires in most cases a combination of methods relying on multiple numerical ages of flood-sediment layers and intervening deposits such as colluvium and soils at each paleoflood site. In some cases dendrochronology can precisely date botanical flood damage to the year or even season, and can provide limiting ages on flood deposits (Ballesteros-Cánovas et al., 2015a; St George and Nielsen, 2003). Numerical dating fix ages to chronologies mainly established by deposit stratigraphy and site-to-site correlations based on deposit characteristics and sequences.

For sedimentary sequences, numerical dating methods aim to establish the timing of individual floods. Radiocarbon dating is the most common numerical dating tool employed in paleohydrologic work (Benito et al., 2010; Harden et al., 2015; Yu et al., 2003), although OSL dating is being increasingly applied (Grodek et al., 2013; Guo et al., 2016; Medialdea et al., 2014). Organic materials such as wood, charcoal, seeds, and leaf fragments are entrained by floods and commonly deposited in conjunction with clastic sediment in slackwater sequences. Additionally, flood deposits may cover vegetation or organic cultural materials, as well as in turn be covered by vegetation and organic detritus. All these types of materials can be radiocarbon dated, thereby providing information on the age of enclosing or bounding flood deposits. Organic materials most likely to provide high fidelity constraints on flood ages are those not likely to have persisted for a long period of time before deposition, such as seeds, fine organic detritus, and twigs. Commonly, however, radiocarbon dating is performed on charcoal contained within flood deposits, which can persist for hundreds of years prior to incorporation within a flood deposit (Blong and Gillespie, 1978). For example, a paleoflood study in southern France by Dezileau et al. (2014) found that 80% radiocarbon dated charcoals yield older ages than the ones expected on the basis of other applied techniques (Cs-137 and Pb-210). In that study, radiocarbon dates on annually produced seeds and twigs provided the best results.

For most studies, it is assumed that radiocarbon ages from detrital material within flood deposits closely approximates the flood date, although the most conservative assumption is that the radiometric date provides a maximum limiting age for the enclosing deposit. This is particularly the case for radiocarbon dates from detrital charcoal. Dating of in situ organic materials, such as charcoal from ground fires between affected surfaces bracketed by flood deposits, or pedogenic carbon between flood deposits, can provide robust constraints on the timing of flood sequences. As for most geologic investigations, dating of multiple organic materials and multiple deposits within a stratigraphic profile can increase the confidence of flood age determinations. The 5730 year half-life of ^{14}C limits radiocarbon dating to deposits less than 40,000 years. Also, radiocarbon dating suffers from significant imprecision for the period AD 1650 to AD 1950 because of the significant fossil fuel burning and introduction of variable amounts of ^{14}C into the atmosphere during the industrial revolution. Post-bomb (between 1945 and 1963) radiocarbon dating is becoming more relevant in paleoflood hydrology for age validation of known floods to related paleostage evidence (Baker et al., 1985; Ely et al., 1992). The atmospheric diffusion of radiocarbon after nuclear testing produced a distinctive ^{14}C spike which provides age control for younger deposits (Wild et al., 1997). Annually produced organic matter, such as twigs, seeds and leaves, yield the most accurate radiocarbon dates, some within 1 year of the known age of the deposit (Ely et al., 1992). However, in arid and semiarid environments, this post-bomb dating is limited due to low decomposition rates of organic debris and persistence of fine organic detritus in the environment.

OSL (Aitken, 1998) is a dating technique which indicates the time elapsed since burial of deposits, principally quartz and feldspar minerals. This approach allows determination of when sediment was last exposed to light ("bleached"). For the purposes of dating sequences of flood deposits, the general assumption is that the sediment was last exposed to light immediately prior to deposition. Sampling and analysis involves several steps of collection and analysis of fine sand-sized sediment from a target deposit without inadvertent exposure to light (Porat, 2006). Recent analytical methods have improved the application OSL dating for alluvial deposits (Murray and Wintle, 2000; Wintle and Murray, 2006), resulting in age uncertainties within 5–10%, even for young deposits (<300 years) (Duller, 2004; Medialdea et al., 2014). Recent research also has highlighted the importance of selecting

suitable sample locations (Rodnight et al., 2006). The technique can be hampered in situations in which (1) the proper species of quartz are not present in the deposits, and (2) for floods where the transported sediment was not bleached by exposure to light, either because of high turbidity levels during the flood or because the flood occurred at night (Medialdea et al., 2014; Smedley and Skirrow, 2020). Developments in OSL instrumentation are reducing the sample size to individual quartz and feldspar grains (Bøtter-Jensen et al., 2000; Duller and Murray, 2000). Under appropriate conditions, OSL dating is an important tool, especially for deposits (1) containing little or no organic materials, (2) older than the range of radiocarbon dating (>40,000 years), or (3) younger than 300 years when radiocarbon dating is imprecise.

Dendrochronology has supported several paleoflood studies due to the well understood responses of tree growth to damage of the bark and wood-forming tissues, buds, and leaves, and to radial growth following partial up-rooting of the trunk (Ballesteros-Cánovas et al., 2015b; McCord, 1996; St George et al., 2002; Therrell and Bialecki, 2015). For situations when flood damage or effects can be related to tree-ring chronologies derived from the affected tree or from established regional chronologies, flood ages can commonly be determined to the specific year, and in some instances a specific season (Jacoby et al., 2008; Sigafoos, 1964). Dendrogeomorphology, a science that uses dendrochronology to study geomorphic changes, is an effective tool to reconstruct flood chronologies in ungaged mountain streams (Bodoque et al., 2015; Ruiz-Villanueva et al., 2013), which can be combined with forest management data, historical archives, long daily precipitation records and sedimentary evidence to reconstruct flash flood activity at a regional scale (Ballesteros-Cánovas et al., 2015a).

Lichenometry can provide numerical dates for flood bars and erosion of alluvial surfaces by floods, particularly over the last 500 years (Innes, 1985). The method allows dating the exposure age of a rock surface (e.g., boulders in a flood bar) based on the relationship between the diameters of the largest lichens with the growth rate of the lichen species (Beschel, 1973). The first application of lichenometry to flood studies was carried out by Gregory (1976) to define and date flood boundaries using lichens present on bedrock and river banks. Subsequent applications to date flood events and phases of recent fluvial activity have been carried out by Harvey et al. (1984), Macklin et al. (1992) Gob et al. (2008), Macklin and Rumsby (2007) and (Foulds et al., 2014). The most common lichen used is genus *Rhizocarpon*, particularly *Rhizocarpon geographicum*, as well as the genus *Xanthoria*. Such dating requires determination of lichenometric growth curves for the specific location and lichen species. These are typically derived from lichen measurements on rock surfaces of known age, commonly tombstones and old monuments (Gob et al., 2003). The convex-upward shape of most associated growth curves is consistent with phases of fast growth of smaller lichens followed by linear growth for larger lichens (Solomina et al., 1994). Most lichenometry studies rely on the assumption that the largest lichens were the first to colonize the rock surface, and typically only a few of the largest lichens are used to establish a growth curve. This assumption can sometimes produce misleading results (Calkin and Ellis, 1984). Lichenometry has not been widely used for paleoflood studies likely because it is limited to boulder bars in mountain streams (Table 1) where other techniques, such as dendrochronology, can be readily applied (Bodoque et al., 2015). Most of the flood events dated by lichenometry were limited to the last 250 years (Foulds and Macklin, 2016). These young ages may indicate a censuring effect due to mortality of the first lichens to colonize the flood boulders (Rosenwinkel et al., 2015).

Radiocarbon and OSL dating can be supplemented with analysis of modern radionuclides such as Cesium-137 and Lead-210 (Dezileau et al., 2014; Ely et al., 1992; Stokes and Walling, 2003; Thorndycraft et al., 2005b). Both of these isotopes were introduced into the atmosphere during nuclear bomb testing in the 1950s. Their presence in flood deposits signifies a post-1950 age and offers a less expensive technique to distinguish modern flood deposits from older ones.

The largest floods usually greatly affect landscapes, commonly leaving a multiple cultural, physical, and botanical records. In particular, assessment of the geomorphic effects of historical floods may help in optimizing the dating strategy and minimize analysis costs. The establishment and growth of riparian vegetation along river corridors is controlled by hydrogeomorphic processes, including flood magnitude and duration, flow velocity and sediment transport fluxes (Osterkarmp and Hupp, 1984). Resulting botanical conditions provide a context for linking flood sediments and geomorphic surfaces with flood timing and magnitude. Archaeological features can be used as an indicator of flood age as well. Along rivers, caves, rock shelters, and flood benches are commonly sites of recurrent human occupation. At such sites, archaeological features may be used to infer floods and date flood episodes. Likewise, more recent human artifacts, such as beer cans (House and Baker, 2001), pottery (Benito et al., 2003a; Huang et al., 2012) can provide numeric age constraints on flood deposits.

2.6 Paleoflood discharge determination

Relating paleoflood evidence to flood discharge is a critical component of most quantitative paleohydrologic studies. The approach for estimating discharge can range from application of simple hydraulic or sediment transport formulae applied to single cross sections to sophisticated two- or even three-dimensional modeling, depending on study objectives, site conditions, and available information and resources. Two primary approaches lead to quantitative estimates of peak discharges from paleoflood deposits: (1) flow estimates derived from paleo-competence evaluated relative to coarse bedload transported by the flood; and (2) flow estimates from hydraulic analysis based on the elevation of deposits relative to local channel geometry.

2.6.1 Paleocompetence

Paleocompetence techniques rely on selective sorting of particles being transported by floods, usually coarse clastic deposits, and are appropriate for estimating the magnitude of singular events (see Jacobson et al., 2016). They have been used commonly for exceptional floods from Pleistocene glacial, volcanic- and landslide-dammed-lake outburst floods (Manville, 2010; Manville et al.,

2007; O'Connor, 1993; Waythomas and Jarrett, 1994), as well as from flash floods from meteorological events (Costa, 1984). Flow competence evaluation is based on selective-entrainment relationships (empirical and physically based equations), usually based on the largest clasts (Carling, 1983; Costa, 1983) providing mean-flow stress, velocity and discharges per unit flow width. Reviews of flow competence methods, including their application and uncertainties, are provided by Maizels (1983); Williams (1983); Williams (1984), Komar (1989), Komar and Carling (1991), Wilcock (1992), O'Connor (1993), Jacobson et al. (2016) and Komar (1996). A recent adaptation of this approach derives from the investigation of Lamb and Fonstad (2010) of a modern canyon-eroding flood in Texas, where they retrodicted flood hydraulics from competence criteria. Their approach has been applied by Sweeney and Roering (2017).

While competence approaches can be used over a broad range of fluvial environments, they typically can only provide imprecise estimates of paleohydraulic values because of the uncertainties in the relations between flow strength variables (generally velocity, shear stress or stream power) and transported clast size. Moreover, discharge can only be estimated for situations in which there is independent knowledge of cross section geometry to apply retrodicted flow-strength variables. Other deficiencies and constraints of the competence approach include difficulties in adequately sampling or characterizing the largest particles, ensuring that measured clasts were indeed transported by water flow (as opposed to debris flow or mass movement), and ensuring that available sources of transported clasts include the entire range that the flow was competent to transport.

2.6.2 Hydraulic analysis

Hydraulic analysis is the basis for discharge estimates for most quantitative paleoflood studies, especially where flood histories are reconstructed from stratigraphic sequences of fine-grained flood deposits. In most analyses, discharge estimates follow from the assumption that the position of paleostage evidence relates closely to the maximum stage attained by an identified flood. This assumption is difficult to verify (Jarrett and England, 2002) and several investigators have reported height differences between flood indicators and actual flood water depth for modern floods (House et al., 2002; Springer and Kite, 1997). In a systematic analysis of flood indicators left by modern floods in North American mountain rivers, Jarrett and England (2002) concluded that flood sediment elevations matched maximum flood stages, especially for deposits left at channel margins. Uncertainties in the fidelity of paleoflood stage evidence to actual maximum stages can be assessed in conjunction with most discharge estimation procedures.

A number of approaches are available to estimate flood discharge from known water surface elevations (Lang et al., 2004; O'Connor and Webb, 1988; Webb and Jarrett, 2002), ranging from simple hydraulic equations to one or multi-dimensional hydraulic modeling. Most paleoflood studies assume one-dimensional flow with calculations based on (1) uniform flow equations (e.g., Manning equation), (2) critical flow conditions (King, 1954), (3) one-dimensional gradually-varied flow models, and (4) two-dimensional, depth averaged hydrodynamic models. As described by Webb and Jarrett (2002), the appropriate approach for a particular site ultimately depends on project objectives and local hydraulic conditions. The use of two-dimensional models is becoming more common, particular for complex reaches (Bohorquez, 2016; Bohorquez et al., 2013; Turzewski et al., 2019).

For all types of hydraulic calculations, the formulae and models are applied to estimated channel geometry and roughness conditions for the time of the flow of interest. For late Holocene floods in bedrock bound fluvial systems, the present valley geometry is commonly assumed to adequately represent the channel conditions at the time of flooding (e.g., Benito et al., 2003a; Ely and Baker, 1985; Greenbaum et al., 2000, 2014a; Harden et al., 2011; O'Connor et al., 1986; Sheffer et al., 2008; Thorndycraft et al., 2005a; Webb et al., 1988). But because channel geometry is the single most important factor in calculating discharge for a specific stage, assessment of this assumption is important for overall uncertainty analysis. Hydraulic analysis of paleofloods in river channels for which flow-boundary geometry is uncertain, requires specific consideration of plausible ranges of channel geometry at the time of flooding (e.g., Larsen and Lamb, 2016). This is the case of alluvial rivers or bedrock bound systems where there has possibly been incision, widening, or alluviation since the flood paleostage evidence was emplaced.

The Mannings equation is applied for uniform flow conditions of straight channels with minimal gradient and regular width (Chow, 1959). In mountain streams with slopes ranging from 0.002 to 0.052 m m^{-1}, Jarrett (1984) developed an equation that uses energy gradient (S) and hydraulic radius (R) to predict an n value of $n = 0.32\ R^{0.38}S^{-0.16}$. The Mannings equation may be re-formulated for estimating velocity and discharge in high-gradient natural channels (Jarrett, 1985). This equation has been applied successfully for discharge estimates based on heights of tree scars and gravel bars (Jarrett, 1985; Rico et al., 2001).

Another special flow condition is that of critical flow (King, 1954), which arises when flow is constricted or subject to substantial slope increase and passes through a state of minimum specific energy [$v/(g \cdot d_c)^{1/2} = 1$]; where v is flow velocity, g is gravitational acceleration ($g = 9.8$ m/s^2), d_c is critical depth] as it funnels through or drops over the channel contraction or slope break. If such conditions can be identified and associated with paleostage evidence, they can provide robust discharge estimates (Bodoque et al., 2011; Webb and Jarrett, 2002). The overriding factor in controlling flow in such stable bedrock conditions is channel geometry. A common situation in bedrock fluvial systems is flood sediment accumulation upstream of constrictions, where flow is controlled by the constriction, promoting upstream hydraulic ponding and deposition of the suspended sediment and bedload. In these situations, the maximum stage evidence can be related to discharge by assuming critical flow in the channel contraction, and assuming that the elevations of the flood deposits in the controlled reach upstream indicate the total mechanical energy of the flow (e.g., Benito et al., 1998; O'Connor et al., 2001). Critical flow conditions are especially common in steep mountain streams, with alternating pool and steep reaches that result in longitudinal accelerations and decelerations through the critical threshold (Bodoque et al., 2011; Grant, 1997). The critical flow method requires the field selection of channel reaches fulfilling the conditions of critical flow (Chow, 1959), but does not depend on the variables such as roughness or slope (Jarrett, 1987; O'Connor and Costa, 1993).

The most common paleoflood analysis situation is that of gradually-varied flow (O'Connor and Webb, 1988; Webb and Jarrett, 2002). River channels are typically irregular in shape and surface roughness, leading to non-uniform flow conditions. In low gradient and larger river systems, critical flow conditions may not be achieved in the absence of significant valley constrictions. The simplest gradually-varied flow analyses assume a steady state (constant discharge) for which flow depth varies with distance but not with time (Chow, 1959). For such situations, calculation of water-surface profiles are based on solution of the conservation of mass and energy equations in their one-dimensional forms. The step-backwater method (Chow, 1959) for gradually-varied water-surface profile computation is the typical approach used to relate paleoflood evidence to discharge (O'Connor and Webb, 1988). Available public-domain computer routines, such as the US Army Corps of Engineers HEC-RAS (Hydrologic Engineering Center, 2010) software, allows for rapid calculation of water-surface profiles for specified discharges, and energy loss coefficients. From these calculations, water-surface elevations are computed by trial and error at specific cross-sections for a given discharge. Multiple analyses can provide synthetic stage-discharge ratings at sites of interest, thus providing a basis for estimating paleoflood discharge from the elevation of a deposit or other high-water evidence. Uncertainties in flow modeling parameters can be evaluated for their resulting influence in paleoflood discharges by testing outcomes of plausible ranges of Mannings n values and possible changes in channel geometry.

Recent paleoflood studies have overcome some specific problems of traditional one dimensional hydraulic models, such as neglecting lateral flow and the flow exchange between the channel and overbank area (Bates and De Roo, 2000) through application of two-dimensional hydrodynamic models (Denlinger et al., 2002). Advances in modeling approaches, computational software, and high-resolution topographic data acquisition now make such models more practical for applied paleoflood studies. Several such two-dimensional models including SRH2D model (Lai, 2008, 2010) have been used extensively for paleoflood studies by the US Bureau of Reclamation (see Bauer and Klinger, 2010). These models typically take advantage if high resolution digital elevation models, such as those derived from terrestrial or airborne laser altimetry, to produce better estimates of flow stage and velocity associated with large flows, particularly in environments of substantial secondary and cross-valley flow currents (Bohorquez et al., 2019; Denlinger et al., 2002). Several open source hydraulic models have been used on paleoflood studies, such as GeoClaw (Turzewski et al., 2019) from the software package Clawpack (Mandli et al., 2016), and Iber (Ballesteros-Cánovas et al., 2016) that simulates unsteady surface flows using a finite volume method with a second-order roe scheme (Bladé et al., 2014). As these hydraulic models and their interfaces advance, coupled with greater availability of high-resolution topography, application of multi-dimensional models to paleoflood studies will become increasingly common.

2.7 Flood frequency analysis

A common objective of paleoflood studies is to provide better estimates of the flood frequency associated to extreme events. Such paleoflood data informed flood frequency analyses can support (1) risk assessments for critical structures such as nuclear facilities, dams, or bridges for which knowledge of infrequent large-magnitude floods is important (Benito et al., 2006; England et al., 2006; Godaire and Bauer, 2013; Levish et al., 1996; O'Connor et al., 1994, 2014) (2) understanding of the recurrence of geomorphically effective flows (Greenbaum et al., 2020; O'Connor et al., 1986), and (3) assessment of non-stationarity in the frequency of large floods due to climate, land-use, or other changes (Benito et al., 2015b; Ely et al., 1993; Harden et al., 2015; Redmond et al., 2002).

Paleoflood analyses have gained credibility in the engineering community because of advances in statistical techniques for taking advantage of non-standard observations of flood magnitude and timing. Non-standard data are those not typically part of gaged or systematic records, including isolated historical observations, interval data (estimates of flood peaks within specified ranges of magnitude and time), paleoflood records, and inferences and observations of discharges that have and not have occurred over specific time intervals (sometimes called paleohydrologic or non-exceedance bounds). Flood frequency analysis approaches evolved from using maximum-likelihood estimators in conjunction with historical and paleoflood data (Cohn et al., 1997; Stedinger and Baker, 1987; Stedinger and Cohn, 1986). Since their origins, the likelihood functions of Stedinger and Cohn (1986) have been incorporated in a Bayesian approach explicitly accounting for paleohydrologic bounds as well as measurement uncertainties (O'Connell et al., 2002). This approach is the basis of FLDFRQ3, a Bureau of Reclamation flood-frequency analysis program that has been used in Bureau of Reclamation dam safety assessments (Swain et al., 2004), and it was also implemented in the software AFINS (Botero and Francés, 2006) that allows using non-systematic information with upper bounded statistical models (Botero and Francés, 2010; Frances and Botero, 2012).

An alternative to maximum-likelihood estimators for incorporating non-standard data in a flood-frequency analysis is the Expected Moments Algorithm (EMA) (Cohn et al., 1997). This approach is nearly as efficient as maximum-likelihood estimation but more widely applicable, including any distribution type amenable to method-of-moments parameter estimation (Cohn et al., 1997). Additionally, EMA is mathematically tractable enabling determination of variance of the estimator (Cohn et al., 2001), thus giving accurate confidence intervals on quantile estimates. The EMA is now implemented in the USGS flood frequency software program, PeakFQ (Flynn et al., 2006; Veilleux et al., 2014) and the US Army Corps of Engineers Software HEC-SSP (Bartles et al., 2016). These programs support flood frequency analyses incorporating paleo- and historical data, an approach now embodied Bulletin 17C (England et al., 2019), the recommended guidelines for flood frequency analysis by federal agencies in the United States.

These new statistical approaches rely on incorporating information on paleohydrologic bounds or "perception thresholds" into the analysis, thereby efficiently accounting for censored geologic or historical information (Fig. 5). Perception thresholds are stages that reflect the range of flows that would have been recorded had they occurred for any given year over a specified time span

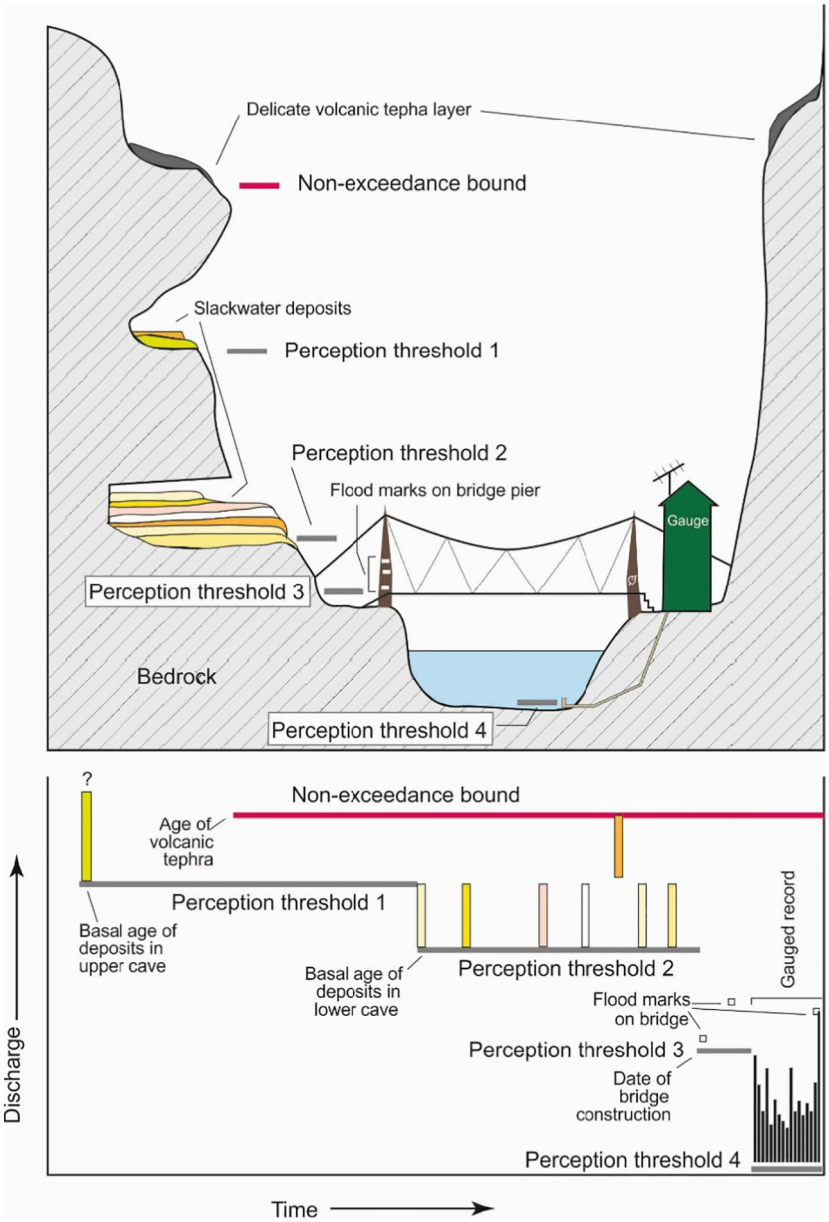

Fig. 5 Hypothetical setting illustrating concept of non-exceedance bounds and perception thresholds, which allow efficient incorporation of paleoflood and historical information into statistical assessment of flood frequency. The non-exceedance bound associated with the volcanic tephra relies on the assumption that the tephra would be removed by erosion if inundated by flooding, thus the lowest elevation of the tephra indicates the maximum possible flood stage since tephra deposition. Perception thresholds 1 and 2 relate to the elevations of the two slackwater deposit sites. The applicable periods of each threshold is the period for which the site is expected to record all floods, which commonly is defined by the oldest preserved stratigraphy at that level (although in some cases, geologic evidence at the site, or from other sites, may indicate longer or shorter periods of applicability). Perception threshold three pertains to flood marks emplaced on a bridge, some prior to establishment of the gaging station. Perception threshold 4 is "0," assuming that the gage records all peak flows. Thus framed, the limits of flood magnitudes (with varying ranges of precision) can in inferred in relation to the bounds for every single year back to the inception of perception threshold 1. The validity of all perception thresholds for flood frequency analysis critically relies on the assumption that all floods exceeding the threshold are recorded.

(England et al., 2019). For example, a high cave in the side of a river valley will only accumulate deposits from large floods high enough to inundate the cave and leave a deposit. In this instance, the perception threshold is the discharge (or stage) associated with inundation, assuming that each inundation results in an individual deposit. Every year, then, the river of interest can be characterized as having a peak discharge either exceeding, or not exceeding, that perception threshold. Such perception thresholds commonly vary with time. For example, the cave might represent a perception threshold for recording extreme floods going back thousands of years, but the last several decades might be accounted for with a lower perception threshold consisting of flood marks on a bridge, assuming that each time flow stage reached the bridge, a mark was made. The end member condition is a typical gaging station, for which the perception threshold is commonly zero, because the peak flow is recorded, and thus precisely known, every

year. Most critical for flood frequency analysis is knowledge of how many floods exceeded a specific perception threshold and the duration of the threshold, not the precise date of each flood. For example, the date of bridge construction could define the beginning of a perception threshold. In a sequence of flood deposits, the duration of the perception threshold migh be based on geochronological evidence for that the site was accumulating flood sediment, commonly based on the age of the oldest deposits. Perception thresholds can have upper bounds, indicating discharges so great that they would not be recorded.

Related but distinct are "non-exceedance bounds," which define intervals for specific discharges that have *not* been exceeded (Levish, 2002). Such bounds are commonly defined on the basis of stable surfaces with no indicators of recent inundation or delicate landscape features unlikely to survive inundation, such as a fine-grained tephra preserved on an outcrop flanking a channel (Fig. 5). The most rigorous non-exceedance assessments account for overtopping depths required for initiating erosion or deposition of the stable terrace surface by considering the shear-stress or stream-power exerted by a range of flows, or by comparing with effects of historical floods (England et al., 2006). Although the lack of flood evidence is not always unequivocal evidence of the absence of flooding, identifying such bounds can greatly constrain the upper limit of discharge for low (<0.01) AEP floods (Botero and Francés, 2010; England et al., 2010; Godaire and Bauer, 2012). Fully understanding the occurrence and magnitude of such low probability floods is important for flood protection and design of sensitive infrastructures such as dams, nuclear power plants, or tailing dams from radioactive mining (Godaire and Bauer, 2012; Levish et al., 1996).

Analyses incorporating non-standard paleoflood and historical flood information improve flood-frequency estimates because they incorporate more and different types of information, typically encompassing much longer time periods than gaged records. Additionally, paleoflood records preferentially provide information on the largest floods, precisely the information necessary to constrain the right-hand tail of the frequency distribution, no matter what frequency distribution is selected. This benefit can be quantified in terms of the equivalent information gain with respect to a record of annual peak flows (Fig. 6). For example, a typical paleoflood record of 1000 years (which is common) containing evidence of only a single flood, provides the equivalent gain of 170–200 years of annual peak flows in estimating the flood discharge associated with the annual exceedance probabilities ranging between 0.01 and 10^{-6}. This represents a gain of 0.17–0.2 "gage station years" for each year of length for the paleoflood record. A 1000-year record containing evidence of 10 floods (which also is common) provides the equivalent of 500 years of annual flow peaks in estimating the 0.01 flood quantile. Considering the rarity and expense of long-duration annual records, paleoflood studies can be a highly efficient means of improving flood frequency estimates, particularly of rare flows.

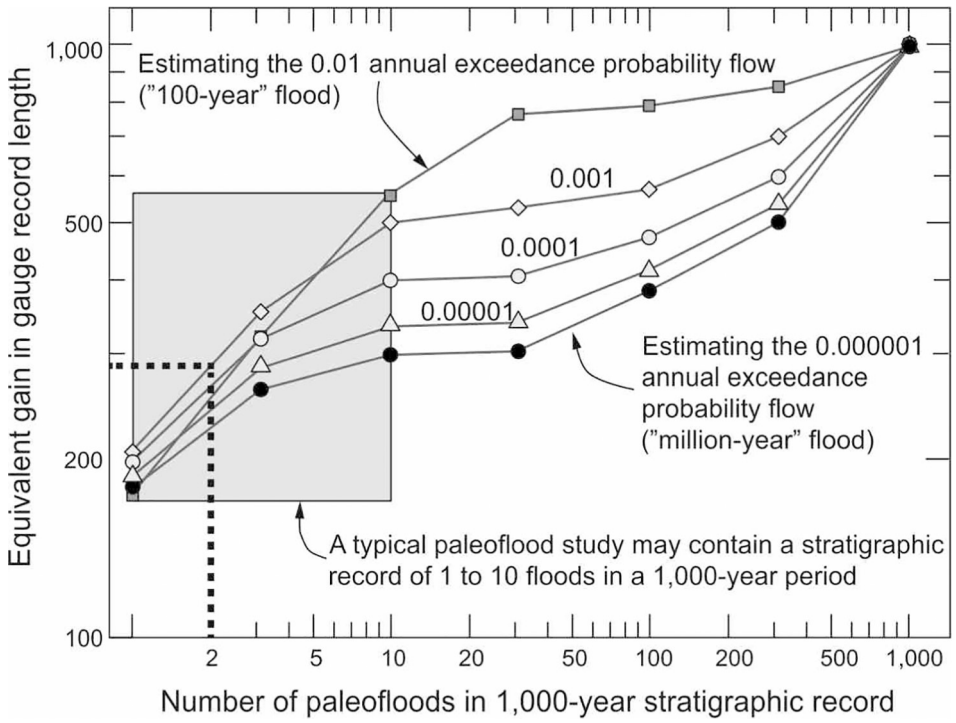

Fig. 6 Gain in flood-frequency information from a paleoflood stratigraphic record of 1000 years, as measured in equivalent years of annual peak flow records (such as would be determined from a gauging station). The gain, in terms of station years or record length, is shown for specific flood quantiles ranging from 0.01 to 10^{-6} annual exceedance probability and as a function of the number of events recorded by stratigraphy. The shaded box bounds the common range of scenarios in which 1000-year stratigraphic records contain information on 1–10 paleofloods, resulting in gains of 150–550 years of equivalent gage record. For example, a stratigraphic record documenting two floods in the last thousand years would be equivalent lengthening the gaged record by nearly 300 years for estimating the 0.001 annual exceedance probability (1000-year) flood. Analysis by Timothy Cohn, from O'Connor JE, Atwater BF, Cohn TA et al. (2014) *Assessing Inundation Hazards to Nuclear Powerplant Sites Using Geologically Extended Histories of Riverine Floods, Tsunamis, and Storm Surges*. Scientific Investigations Report 2014–5207. U.S. Geological Survey.

Use of these paleoflood approaches, however, requires understanding the uncertainties and sensitivities. Results are sensitive to the values of the measured peaks and the assigned values of the perception thresholds and non-exceedance bounds. Consequently, defining and characterizing perception thresholds and bounds have been emphasized increasingly in recent paleoflood studies (e.g., Harden et al., 2011). Additional statistical issues and uncertainties related to the use of paleoflood information in flood frequency analysis, such as non-stationarity, are discussed in O'Connor et al. (2014). Paleoflood record stationarity from censored samples (systematic and/or non-systematic) can be checked using a Poisson test (Lang et al., 1999). This test assumes that the flood series can be described by a homogenous Poisson process. The 95% tolerance interval of the accumulative number of floods above a threshold, or censored, level is computed. Stationary flood series are those remaining within the 95% tolerance interval (e.g., Thorndycraft et al., 2005a; Fig. 7B). Non-stationary models may be implemented with non-systematic paleoflood data, once the driving covariate (e.g., hydro-climatic index) on parameter change is established (Machado et al., 2015).

3 A paleoflood case study: The Llobregat River

A paleoflood analysis on the Llobregat River at Monistrol de Montserrat (~50 km northwest of Barcelona, NE Spain) provides a good example of the analyses required to use paleoflood discharge estimates to flood hazard assessment. This summary is derived from the complete report of Thorndycraft et al. (2005a).

The Llobregat River has a typically Mediterranean climate with extreme seasonal variations. Flood peaks are sometimes 100 times greater than the mean annual discharge of 21 $m^3 s^{-1}$. In the studied reach (2.5 km in length) the channel drains 3370 km^2 and is confined to a bedrock canyon with vertical walls as the river trends south through Eocene conglomerates. Slackwater flood sediments have been deposited and preserved in six valley side rock alcoves developed within the predominantly horizontal rock strata. Stratigraphic and sedimentological analyses of the deposits were carried out both in the field and the laboratory, supported by 80 cm × 50 cm sediment peels of the stratigraphic profiles (Thorndycraft et al., 2005a). Flood chronology was determined by radiocarbon and Cesium-137 dating (Thorndycraft et al., 2005b).

The slackwater flood deposits of the Llobregat River are composed predominantly of very fine to fine-grained sand with parallel laminations alternating with climbing ripples in drift and climbing ripples in phase. In total, 46 individual flood units were identified in six stratigraphic profiles. The number of flood units preserved at the different sites reflects relationships between flood magnitude and frequency, with greater numbers of modern flood events located in the lower elevation alcoves (relative to the channel bottom) such as Alcove E. The highest elevation site, Alcove C (Fig. 7A), contains a single flood unit with a radiocarbon date of cal. AD 1516–1642. This date and the exceptional altitude (16 m above the river bed), when cross-referenced with the documentary flood record from the Llobregat River, imply that this unit was most likely deposited by the 1617 flood (Thorndycraft et al., 2005a), the largest flood of the last seven centuries according to historical flood observations. The next oldest dated sediments are from Alcove F (Fig. 7A), with the basal flood unit (F1) dated to 185 ± 55 BP (cal. AD 1790 ± 92). This date is in a range of poor radiocarbon dating resolution (Trumbore, 2000); it is likely, however, that the deposit dates to the 19th century. The best dating control for the recent slackwater sequences was provided by ^{137}Cs analysis, as the most recent sediments could be assigned only as modern, based on the radiocarbon results alone. Alcove E contains the most modern flood units, with 10 units post-dating the mid-1950s, as signaled by the presence of anthropogenic ^{137}Cs. The stratigraphy and geochronology of slightly higher Alcoves D, G and H indicates that only two or three post mid-50s floods reached these levels.

Discharges associated with the flood units at each site were estimated by computing water surface profiles for hypothetical series of specified discharges run using the HEC-RAS one-dimensional model. The initial water surface elevation was set at a constricted section 2.5 km (Cairat Gap) downstream of the studied reach, for which critical flow was assumed. These calculated water-surface profiles were compared to the elevations of the flood deposits along the Monistrol study reach (Fig. 7A). For this reach, the calculated water-surface profile for a discharge of 6200 $m^3 s^{-1}$ matches the highest slackwater deposits of the C1 unit (Fig. 7A). A more conservative estimate of the discharge associated with this deposit elevation results from consideration of the calculated energy surfaces (stage plus velocity head), recognizing that some deposits will be emplaced at higher elevations than the cross-sectional average water-surface stage because of the two-dimensional nature of flood flows. In this case, a discharge of 4680 $m^3 s^{-1}$ results in an energy surface matching the deposit elevation and was considered to provide a more accurate estimate of the emplacing discharge (Thorndycraft et al., 2005a). The ranges of estimated discharges required for floodwaters to reach either the base or the roof of the alcoves are indicated in Fig. 7A. There are a number of alcoves (D, F and G) along the study reaches that require discharges in excess of 2000 $m^3 s^{-1}$ to overtop the flood sediments. Only two alcoves (E and H) were inundated by the June 2000 flood event, having a measured peak discharge of 1200 $m^3 s^{-1}$, where maximum stage was marked by silt lines on the gorge wall and fissures in the rock filled with debris (Fig. 7A). The slackwater flood deposits and associated paleodischarge estimates provide strong evidence of ancient floods with discharges greater than those recorded in the gage station ~3 km upstream for which measurements extend back to 1913.

The paleoflood records from this reach were combined with the nearby gaged record to estimate flood frequency. For this analysis the information considered included the annual flood peaks from the 1913–2000 gaged record, the 12 paleofloods since AD 1790 (radiocarbon dated at site F1), which also gives the lower bounds or perception levels, and an upper bound premised on the inference (from historical accounts) that the flood discharge estimated for the 1617 flood has not been subsequently exceeded. Timing and discharges of paleoflood and gaged records are represented in Fig. 7C (modified from Botero, 2006). The shaded area indicates the time and discharge domain of the perception levels, here specified to increase as the flood deposits accumulated—only

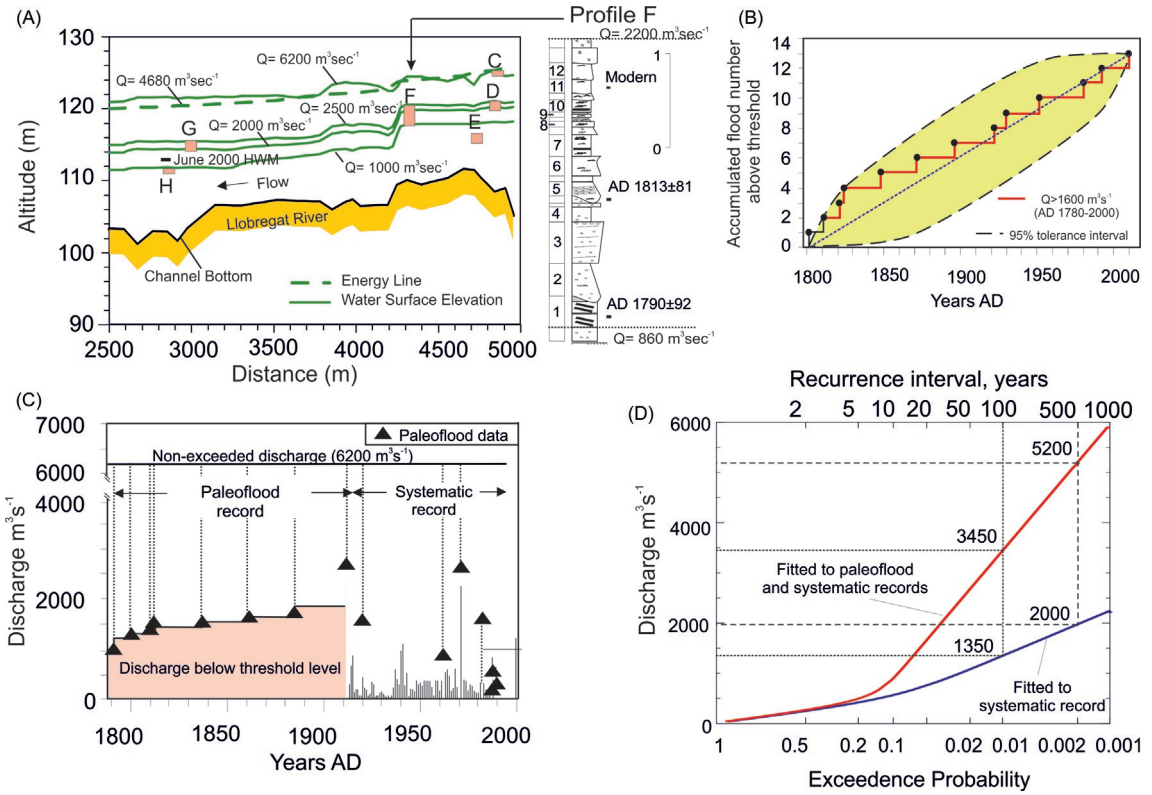

Fig. 7 Llobregat paleoflood case study based on data after Thorndycraft et al. (2005a). (A) Calculated water surface and energy line elevations (in *green*) for selected discharges related to the elevations of mapped slackwater flood deposits at alcoves C-H along—the Monistrol study reach. Also shown is the elevation of debris and silt lines left above Alcove H by the June 2000 flood. This modern flood data was used to calibrate the hydraulic model at this reach. (B) Poisson test on the time flood sequence in the Llobregat record for the period 1790–2003, for floods exceeding a discharge threshold of 980 $m^3 s^{-1}$. The dotted line shows equal exceedance probability over the period 1780–2000. Note that the flood series (red line connecting points) remain within the 95% tolerance interval (enveloped curves), i.e., annual exceedance probability of the 13 paleoflood events is stationary for this flood magnitude. (C) Organization of historical systematic and paleoflood data for the Llobregat River at Monistrol with respect to inferred perception levels and non-exceedance bounds in support of flood frequency analysis (modified from Botero BA (2006) *Estimación de Crecidas de alto periodo de retorno mediante funciones de distribución con límite superior e información no sistemática*. Polytechnical University of Valencia: Valencia, pp. 223). (D) Two component extreme-value distribution fitted with (1) systematic data and (2) systematic and paleoflood data. Discharge values in cubic meters per second are shown for return intervals of 500 years and 100 years based on the two frequency analyses. Discharge values from the distribution fitted with paleoflood data are more than twice those based only on the systematic flood series. Moreover, the 500-year discharge value of 5200 $m^3 s^{-1}$ is on the same order of magnitude of a discharge of 4680–6200 $m^3 s^{-1}$ estimated for the AD 1617 flood, despite this event not being included in the flood frequency analysis. *HWM*, high water mark; *Q*, discharge.

floods overtopping a sequence of flood deposits can leave a record (Fig. 7C). Seven floods with minimum discharges of 860–2200 $m^3 s^{-1}$ were deposited in Alcove F prior to the gage record. In the 20th century, four floods exceeded 1600 $m^3 s^{-1}$ (1913, 1919, 1971 and 1982) and at least two reached 2500 $m^3 s^{-1}$ (likely 1913 and 1971 floods). Tentative ages were assigned to the paleoflood units (and corresponding censoring thresholds) based on documentary records of known floods (Fig. 7C). Lang's stationarity test was passed for the Llobregat combined flood record covering the period 1790–2003 with a lower threshold discharge of 980 $m^3 s^{-1}$ (Fig. 7B).

Multiple probability distributions functions were fit to the reconstructed flood data series with statistical parameters estimated by the maximum likelihood method (Stedinger and Cohn, 1986). The distribution function with the best fit to the data was the Two Component Extreme Value distribution (Fig. 7D). The incorporation of the paleoflood data into the frequency analysis increases the flood quantile estimates for the Llobregat River substantially—by a factor of two for annual exceedance probabilities less than 0.05 (Fig. 7D). The largest paleoflood discharge (Alcove C, likely of 1617 flood) is associated with a return period of ~500 years, whereas one of the two largest floods of the 20th century (1971) represents a return period of c. 50-year flood (Fig. 7D). The fitted distribution based on paleoflood and systematic data shows a characteristic dog-leg shape commonly associated with flood populations derived from of a mixture of two or more flood generation processes (Alila and Mtiraoui, 2002). Differences between the populations may be the result of a number of factors, including seasonal variations in the flood-producing mechanisms (such as autumn floods instead of winter-spring floods) and changes in weather patterns resulting from low-frequency climate shifts.

This paleoflood analysis illustrates the common situation of the gaging station data not being fully representative of the low probability floods (300–500-year return period) affecting a river reach. Here, the hydrological series is too short to make informed

decisions regarding flood risk for infrequent floods and that paleoflood data provide valuable and quantitative information for flood hazard mapping as requested in the European Flood Directive.

4 Concluding remarks and perspectives

This article has reviewed techniques and approaches for obtaining quantitative information on specific past floods from the geologic record, describing strengths and limitations of various analysis methods. Paleoflood hydrology has gained recognition among hydrologists, statasticians, and engineers as a valuable tool to extend flood series data back beyond the gage record and thereby provide better estimates of the frequency and magnitude of rare floods. The extension of the flood record of rare floods to centuries and even millennia is widely applicable for scientific and engineering problems, including (1) flood hazard assessments based on flood frequency analyses (Benito et al., 2010; Harden et al., 2011), and (2) determination of maximum flood discharge over a specific period of time (Cloete et al., 2018; Enzel et al., 1993) for hydrologic risk analysis of critical facilities (such as dams and wastewater facilities and power plants; Bauer and Klinger, 2010; Godaire and Bauer, 2013; Greenbaum et al., 2014a; Levish et al., 1996; Machado et al., 2017). Considering ongoing discussions as to how climate change may affect flood occurrence at regional and local scales, paleoflood hydrology can provide a perspective by showing how flood magnitude and frequency has responded to past climate shifts over millennia time scales (Benito et al., 2015a,b; Ely et al., 1993; Harden et al., 2015; Knox, 2000), and to different specific modes of atmospheric and oceanic circulation patterns (Ballesteros-Cánovas et al., 2019; Benito et al., 2015a,b; Ely et al., 1993). Additionally, floods in dryland environments have been recognized as a fundamental water resource for human systems and ecosystems (Grodek et al., 2020), opening new paleoflood research directions assessing long-term water infiltration into alluvial aquifers (Benito et al., 2011a,b; Greenbaum et al., 2002; Grodek et al., 2013). Advances in paleoflood science are expected to benefit from improvements in geochronological methods and better and more readily available topographic information, which support higher resolution flow modeling.

More analysis tools are now being applied to paleoflood research, thus expanding the settings providing flood records. Lakes, alluvial floodplains, and delta settings, commonly analyzed with geophysical and geochemical core measurement techniques, are providing flood records (Corella et al., 2016; Jones et al., 2012; Toonen, 2015; Wilhelm et al., 2016). New techniques exploring tree physiological response to floods are also opening new ground to flood reconstructions (Ballesteros-Cánovas et al., 2010; St George et al., 2002; Wertz et al., 2013). Multidisciplinary studies combining marine and lake records with more conventional slackwater flood deposit records can provide further insight into flood frequency and magnitude in relation to climate and environmental changes at basin scales. Other areas ripe for investigation include better understanding of relations between sedimentary sequences and local hydraulics that can lead to a better estimation of the water depth and flow energy required to reproduce the sedimentary structures, methods to relate suspended sediment concentration with flood unit thickness, and techniques for obtaining information about flood hydrograph characteristics from deposit characteristics.

Acknowledgments

GB was funded by the Ministry of Science, Innovation and Universities through the project "Assessment and modelling eco-hydrological and sedimentary responses in Mediterranean catchments for climate and environmental change adaptation" EPHIMED (CGL2017-86839-C3-1-R) co-financed with FEDER funds. Recent USGS paleoflood studies have been in collaboration with U.S. Nuclear Regulatory Commission, U.S. Bureau of Reclamation, and the U.S. Army Corps of Engineers.

References

Aitken MJ (1998) *An Introduction to Optical Dating: The Dating of Quaternary Sediments by the Use of Photon-Stimulated Luminescence*. Oxford: Oxford University Press. 267 pp.

Alila Y and Mtiraoui A (2002) Implications of heterogeneous flood-frequency distributions on traditional stream-discharge prediction techniques. *Hydrological Processes* 16: 1065–1084.

Amann B, Szidat S, and Grosjean M (2015) A millennial-long record of warm season precipitation and flood frequency for the North-western Alps inferred from varved lake sediments: Implications for the future. *Quaternary Science Reviews* 115: 89–100.

Baker VR (2008) Paleoflood hydrology: Origin, progress, prospects. *Geomorphology* 101: 1–13.

Baker VR (2020) Global megaflood paleohydrology. In: Herget J and Fontana A (eds.) *Palaeohydrology: Traces, Tracks and Trails of Extreme Events*, pp. 3–28. Cham: Springer International Publishing.

Baker VR, Kochel RC, Patton PC, and Pickup G (1983) Palaeohydrologic analysis of Holocene flood slack-water sediments. *Special Publication - International Association of Sedimentologists* 6: 229–239.

Baker VR, Pickup G, and Polach HA (1985) Radiocarbon dating of flood events, Katherine Gorge, Northern Territory, Australia. *Geology* 13: 344–347.

Baker VR, Webb RH, and House PK (2002) The scientific, and societal value of paleoflood hydrology. In: House PK, Webb RH, Baker VR, and Levish DR (eds.) *Ancient Floods, Modern Hazards: Principles and Applications of Paleoflood Hydrology*, pp. 1–19. Washington, DC: American Geophysical Union.

Ballesteros-Cánovas JA, Stoffel M, Bodoque JM, et al. (2010) Changes in wood anatomy in tree rings of Pinus pinaster Ait. Following wounding by flash floods. *Tree-Ring Research* 66: 93–103.

Ballesteros-Cánovas JA, Rodriguez-Morata C, Garofano-Gomez V, et al. (2015a) Unravelling past flash flood activity in a forested mountain catchment of the Spanish Central System. *Journal of Hydrology* 529: 468–479.

Ballesteros-Cánovas JA, Stoffel M, St George S, and Hirschboeck K (2015b) A review of flood records from tree rings. *Progress in Physical Geography* 39: 794–816.

Ballesteros-Cánovas JA, Stoffel M, Spyt B, et al. (2016) Paleoflood discharge reconstruction in Tatra Mountain streams. *Geomorphology* 272: 92–101.
Ballesteros-Cánovas JA, Stoffel M, Benito G, et al. (2019) On the extraordinary winter flood episode over the North Atlantic Basin in 1936. *Annals of the New York Academy of Sciences* 1436: 206–216.
Bartles M, Brunner G, Fleming M, et al. (2016) *HEC-SSP Statistical Software Package Version 2.1, CPD-86*. Davis, CA: U.S. Army Corps of Engineers, Institute for Water Resources. 379 pp.
Bates PD and De Roo APJ (2000) A simple raster-based model for flood inundation simulation. *Journal of Hydrology* 236: 54–77.
Bauer T and Klinger RE (2010) *Evaluation of Paleoflood Peak Discharge Estimates in Hydrologic Hazard Studies*. Denver, CO: U.S. Bureau of Reclamation.
Beebee R and O'Connor J (2013) The outhouse flood: A large Holocene flood on the Lower Deschutes River, Oregon. In: O'Connor JE and Grant GE (eds.) *A Peculiar River*, pp. 147–166. Washington DC: American Geophysical Union.
Benito G and Díez-Herrero A (2015) Palaeoflood hydrology: Reconstructing rare events and extreme flood discharges. In: Paron P and Di Baldassarre G (eds.) *Hydro-Meteorological Hazards, Risks and Disasters*, pp. 65–104. Amsterdam: Elsevier.
Benito G and Thorndycraft VR (2005) Palaeoflood hydrology and its role in applied hydrological sciences. *Journal of Hydrology* 313: 3–15.
Benito G and Thorndycraft VR (2020) Catastrophic glacial-lake outburst flooding of the Patagonian Ice Sheet. *Earth-Science Reviews* 200: 102996.
Benito G, Grodek T, and Enzel Y (1998) The geomorphic and hydrologic impacts of the catastrophic failure of flood-control-dams the 1996-Biescas flood (Central Pyrenees, Spain). *Zeitschrift für Geomorphologie* 42: 417–437.
Benito G, Díez-Herrero A, and Fernández De Villalta M (2003a) Magnitude and frequency of flooding in the Tagus basin (Central Spain) over the last millennium. *Climatic Change* 58: 171–192.
Benito G, Sanchez-Moya Y, and Sopena A (2003b) Sedimentology of high-stage flood deposits of the Tagus River, Central Spain. *Sedimentary Geology* 157: 107–132.
Benito G, Sopena A, Sanchez-Moya Y, et al. (2003c) Palaeoflood record of the Tagus River (Central Spain) during the Late Pleistocene and Holocene. *Quaternary Science Reviews* 22: 1737–1756.
Benito G, Rico M, Thorndycraft VR, et al. (2006) Palaeoflood records applied to assess dam safety in SE Spain. In: Ferreira R, Alves E, Leal J, and Cardoso A (eds.) *River Flow 2006*, pp. 2113–2120. London: Taylor & Francis Group.
Benito G, Rico M, Sánchez-Moya Y, et al. (2010) The impact of late Holocene climatic variability and land use change on the flood hydrology of the Guadalentín River, southeast Spain. *Global and Planetary Change* 70: 53–63.
Benito G, Botero BA, Thorndycraft VR, et al. (2011a) Rainfall-runoff modelling and palaeoflood hydrology applied to reconstruct centennial scale records of flooding and aquifer recharge in ungauged ephemeral rivers. *Hydrology and Earth System Sciences* 15: 1185–1196.
Benito G, Thorndycraft VR, Rico MT, et al. (2011b) Hydrological response of a dryland ephemeral river to southern African climatic variability during the last millennium. *Quaternary Research* 75: 471–482.
Benito G, Thorndycraft VR, Machado MJ, et al. (2014) Magnitud y frecuencia de inundaciones Holocenas generadas por vaciamiento de lagos glaciares en el Rio Baker, Campo de Hielo, Patagonico Norte, Chile. In: Schnabel S and Gómez Gutiérrez A (eds.) *Avances de la Geomorfolog/a en España 2012–2014*, pp. 24–27. Cáceres: Sociedad Española de Geomorfología.
Benito G, Macklin MG, Panin A, et al. (2015a) Recurring flood distribution patterns related to short-term Holocene climatic variability. *Scientific Reports* 5: 16398.
Benito G, Macklin MG, Zielhofer C, et al. (2015b) Holocene flooding and climate Change in the Mediterranean. *Catena* 130: 13–33.
Benito G, Sanchez-Moya Y, Medialdea A, et al. (2020) Extreme floods in small Mediterranean catchments: Long-term response to climate variability and change. *Water* 12: 1008.
Beschel RE (1973) Lichens as a measure of the age of recent moraines. *Arctic and Alpine Research* 5: 303–309.
Bladé E, Cea L, Corestein G, et al. (2014) Iber: Herramienta de simulación numérica del flujo en ríos. *Revista Internacional de Métodos Numéricos para Cálculo y Diseño en Ingenier/a* 30: 1–10.
Blong RJ and Gillespie R (1978) Fluvially transported charcoal gives erroneous 14C ages for recent deposits. *Nature* 271: 739–741.
Bodoque JM, Eguibar MA, Díez-Herrero A, et al. (2011) Can the discharge of a hyperconcentrated flow be estimated from paleoflood evidence? *Water Resources Research* 47. https://doi.org/10.1029/2011WR010380.
Bodoque JM, Diez-Herrero A, Eguibar MA, et al. (2015) Challenges in paleoflood hydrology applied to risk analysis in mountainous watersheds—A review. *Journal of Hydrology* 529: 449–467.
Bohorquez P (2016) Paleohydraulic Reconstruction of Modern Large Floods at Subcritical Speed in a Confined Valley: Proof of Concept. *Water* 8: 567. https://doi.org/10.3390/w8120567.
Bohorquez P, Garcia-Garcia F, Perez-Valera F, and Martinez-Sanchez C (2013) Unsteady two-dimensional paleohydraulic reconstruction of extreme floods over the last 4000 yr in Segura River, southeast Spain. *Journal of Hydrology* 477: 229–239.
Bohorquez P, Jimenez-Ruiz PJ, and Carling PA (2019) Revisiting the dynamics of catastrophic late Pleistocene glacial-lake drainage, Altai Mountains, central Asia. *Earth-Science Reviews* 197: 102892.
Botero BA (2006) *Estimación de Crecidas de alto periodo de retorno mediante funciones de distribución con límite superior e información no sistemática*. Valencia: Polytechnical University of Valencia223.
Botero, B.A., Francés, F., 2006. *AFINS Version 2.0-Análisis de Frecuencia de Extremos con Información Sistemática y No Sistemática. Research Group on Hydraulic and Hydrology*. Department of Hydraulic Engineering and Environment, Politechnical University of Valencia: Valencia.
Botero BA and Francés F (2010) Estimation of high return period flood quantiles using additional non-systematic information with upper bounded statistical models. *Hydrology and Earth System Sciences* 14: 2617–2628.
Bøtter-Jensen L, Bulur E, Duller GAT, and Murray AS (2000) Advances in luminescence instrument systems. *Radiation Measurements* 32: 523–528.
Calkin PE and Ellis JM (1984) Development and Application of a Lichenometric Dating Curve, Brooks Range, Alaska. In: Mahaney WC (ed.) *Developments in Palaeontology and Stratigraphy*, pp. 227–246. Elsevier.
Carling PA (1983) Threshold of coarse sediment transport in broad and narrow natural streams. *Earth Surface Processes and Landforms* 8: 1–18.
Chatters JC and Hoover KA (1986) Changing late Holocene flooding frequencies on the Columbia River, Washington. *Quaternary Research* 26: 309–320.
Chatters JC and Hoover KA (1992) Response of the Columbia River fluvial system to Holocene climatic change. *Quaternary Research* 37: 42–59.
Chow VT (1959) *Open-Channel Hydraulics*. New York: McGraw-Hill. 680 pp.
Cloete G, Benito G, Grodek T, et al. (2018) Analyses of the magnitude and frequency of a 400-year flood record in the Fish River Basin, Namibia. *Geomorphology* 320: 1–17.
Cohn TA, Lane WL, and Baier WG (1997) An algorithm for computing moments-based flood quantile estimates when historical flood information is available. *Water Resources Research* 33: 2089–2096.
Cohn TA, Lane WL, and Stedinger JR (2001) Confidence intervals for expected moments algorithm flood quantile estimates. *Water Resources Research* 37: 1695–1706.
Corella JP, Valero-Garcés BL, Vicente-Serrano SM, et al. (2016) Three millennia of heavy rainfalls in Western Mediterranean: Frequency, seasonality and atmospheric drivers. *Scientific Reports* 6: 38206.
Costa JE (1983) Paleohydraulic reconstruction of flash- flood peaks from boulder deposits in the Colorado Front Range. *Geological Society of America Bulletin* 94: 986–1004.
Costa JE (1984) Physical Geomorphology of Debris Flows. In: Costa JE and Fleisher PJ (eds.) *Developments and Applications of Geomorphology*, pp. 268–317. Berlin Heidelberg, Berlin, Heidelberg: Springer.
Davis L, Lombardi R, Sterart CL, Stinchcomb GE, Forman SL, Yaw M, and Jawdy CM (2019) Characterizing extreme floods on the middle Tennessee River, Alabama (USA) using a paleoflood chronology. In: *American Geophysical Union Annual Meeting,* San Francisco, CA, December 9–12, 2019, N44F-04.

Denlinger RP, O'Connell DRH, and House PK (2002) Robust determination of stage and discharge: An example form an extreme flood on the Verde River, Arizona. In: House PK, Webb RH, Baker VR, and Levish DR (eds.) *Ancient Floods, Modern Hazards: Principles and Applications of Paleoflood Hydrology*, pp. 127–146. Washington DC: American Geophysical Union.
Denniston RF and Luetscher M (2017) Speleothems as high-resolution paleoflood archives. *Quaternary Science Reviews* 170: 1–13.
Dezileau L, Terrier B, Berger JF, et al. (2014) A multidating approach applied to historical slackwater flood deposits of the Gardon River, SE France. *Geomorphology* 214: 56–68.
Duller GAT (2004) Luminescence dating of quaternary sediments: Recent advances. *Journal of Quaternary Science* 19: 183–192.
Duller G and Murray A (2000) Luminescence dating of sediments using individual mineral grains. *Geologos* 5: 88–106.
Dussaillant A, Benito G, Buytaert W, et al. (2010) Repeated glacial-lake outburst floods in Patagonia: An increasing hazard? *Natural Hazards* 54: 469–481.
Ely LL and Baker VR (1985) Reconstructing paleoflood hydrology with slackwater deposits - Verde River, Arizona. *Physical Geography* 6: 103–126.
Ely LL, Webb RH, and Enzel Y (1992) Accuracy of post-bomb 137Cs and 14C in dating fluvial deposits. *Quaternary Research* 38: 196–204.
Ely LL, Enzel Y, Baker VR, and Cayan DR (1993) A 5000-year record of extreme floods and climate change in the southwestern United States. *Science* 262: 410–412.
Ely LL, Enzel Y, Baker VR, et al. (1996) Changes in the magnitude and frequency of late Holocene monsoon floods on the Narmada River, central India. *Geological Society of America Bulletin* 108: 1134–1148.
England JF Jr., Klawon JE, Klinger RE, and Bauer TR (2006) *Flood Hazard Study*. Colorado: Pueblo Dam.
England JF Jr., Godaire JE, Klinger RE, et al. (2010) Paleohydrologic bounds and extreme flood frequency of the Upper Arkansas River, Colorado, USA. *Geomorphology* 124: 1–16.
England Jr., J.F., Cohn, T.A., Faber, B.A. et al., 2019. *Guidelines for determining flood flow frequency—Bulletin 17C*. 4-B5, Reston, VA.
Enzel Y (1992) Flood frequency of the Mojave River and the Formation of Late Holocene Playa Lakes, Southern California, USA. *The Holocene* 2: 11–18.
Enzel Y, Ely LL, House PK, et al. (1993) Paleoflood evidence for a natural upper bound to flood magnitudes in the Colorado River basin. *Water Resources Research* 29: 2287–2297.
Enzel Y, Ely LL, Martinezgoytre J, and Vivian RG (1994) Paleofloods and a dam-failure flood on the Virgin River, Utah and Arizona. *Journal of Hydrology* 153: 291–315.
Erskine W and Peacock C (2002) Late Holocene flood plain development following a cataclysmic flood. *IAHS-AISH Publication* 276: 177–184.
Fan L, Huang CC, Pang J, et al. (2015) Sedimentary records of palaeofloods in the Wubu Reach along the Jin-Shaan gorges of the middle Yellow River, China. *Quaternary International* 380-381: 368–376.
Feinberg JM, Lascu I, Lima EA, et al. (2019) Magnetic detection of paleoflood layers in stalagmites and implications for historical land use changes. *Earth and Planetary Science Letters* 530: 115946.
Flynn KM, Kirby WH, and Hummel PR (2006) *User's Manual for Program PeakFQ Annual Flood-Frequency Analysis Using Bulletin 17B Guidelines*. U.S. Geological Survey. 42 pp.
Foulds SA and Macklin MG (2016) A hydrogeomorphic assessment of twenty-first century floods in the UK. *Earth Surface Processes and Landforms* 41: 256–270.
Foulds SA, Griffiths HM, Macklin MG, and Brewer PA (2014) Geomorphological records of extreme floods and their relationship to decadal-scale climate change. *Geomorphology* 216: 193–207.
Frances F and Botero BA (2012) Probable Maximum Flood estimation using upper bounded statistical models and its effect on high return period quantiles. In: EscuderBueno I, Matheu E, Altarejos-Garcia L, and Castillo-Rodriguez JT (eds.) *Proceedings of the 3rd International Forum on Risk Analysis, Dam Safety Dam Security and Critical Infrastructure Management (3iwrdd-forum)*, pp. 323–328. Valencia: Taylor & Francis Group.
Garcia-Garcia F, Bohorquez P, Martinez-Sanchez C, et al. (2013) Stratigraphic architecture and alluvial geoarchaeology of an ephemeral fluvial infilling: Climatic versus anthropogenic factors controlling the Holocene fluvial evolution in southeastern Spain drylands. *Catena* 104: 272–279.
Garrote J, Diez-Herrero A, Genova M, et al. (2018) Improving flood maps in ungauged fluvial basins with dendrogeomorphological data. An example from the Caldera de Taburiente National Park (Canary Islands, Spain). *Geosciences* 8: 300.
Gob F, Petit F, Bravard JP, et al. (2003) Lichenometric application to historical and subrecent dynamics and sediment transport of a Corsican stream (Figarella River—France). *Quaternary Science Reviews* 22: 2111–2124.
Gob F, Jacob N, Bravard J-P, and Petit F (2008) The value of lichenometry and historical archives in assessing the incision of submediterranean rivers from the Little Ice Age in the Ardèche and upper Loire (France). *Geomorphology* 94: 170–183.
Godaire JE and Bauer TR (2012) *Paleoflood study, North Fork Red River basin near Altus dam, Oklahoma*. Denver, Colo: U.S. Department of Interior, Bureau of Reclamation.
Godaire JE and Bauer TR (2013) *Paleoflood Study on the Rio Chama Near El Vado Dam, New Mexico*. Denver, Colo: U.S. Department of Interior, Bureau of Reclamation.
Gonzalez-Lemos S, Müller W, Pisonero J, et al. (2015) Holocene flood frequency reconstruction from speleothems in northern Spain. *Quaternary Science Reviews* 127: 129–140.
Goodbred SL Jr. and Kuehl SA (2000) Enormous Ganges-Brahmaputra sediment discharge during strengthened early Holocene monsoon. *Geology* 28: 1083–1086.
Goswami K, Rawat M, Jaiswal MK, and Kale VS (2019) Luminescence chronology of late-Holocene palaeofloods in the upper Kaveri basin, India: An insight into the climate–flood relationship. *The Holocene* 29: 1094–1104.
Grant GE (1997) Critical flow constrains flow hydraulics in mobile-bed streams: A new hypothesis. *Water Resources Research* 33: 349–358.
Greenbaum N, Schick AP, and Baker VR (2000) The palaeoflood record of a hyperarid catchment, Nahal Zin, Negev Desert, Israel. *Earth Surface Processes and Landforms* 25: 951–971.
Greenbaum N, Schwartz U, Schick AP, and Enzel Y (2002) Palaeofloods and the estimation of long-term transmission losses and recharge to the Lower Nahal Zin alluvial aquifer, Negev Desert, Israel. In: House PK, Webb RH, Baker VR, and Levish DR (eds.) *Ancient Floods, Modern Hazards: Principles and Applications of Paleoflood Hydrology*, pp. 311–328. Washington, DC: American Geophysical Union.
Greenbaum N, Porat N, Rhodes E, and Enzel Y (2006) Large floods during late Oxygen Isotope Stage 3, southern Negev desert, Israel. *Quaternary Science Reviews* 25: 704–719.
Greenbaum N, Harden TM, Baker VR, et al. (2014a) A 2000 year natural record of magnitudes and frequencies for the largest Upper Colorado River floods near Moab, Utah. *Water Resources Research* 50: 5249–5269.
Greenbaum N, Schwartz U, Benito G, et al. (2014b) Paleohydrology of extraordinary floods along the Swakop River at the margin of the Namib Desert and their paleoclimate implications. *Quaternary Science Reviews* 103: 153–169.
Greenbaum N, Schwartz U, Carling P, et al. (2020) Frequency of boulders transport during large floods in hyperarid areas using paleoflood analysis – An example from the Negev Desert, Israel. *Earth-Science Reviews* 202: 103086.
Gregory KJ (1976) Lichens and the determination of river channel capacity. *Earth Surface Processes* 1: 273–285.
Grodek T, Benito G, Botero BA, et al. (2013) The last millennium largest floods in the hyperarid Kuiseb River basin, Namib Desert. *Journal of Quaternary Science* 28: 258–270.
Grodek T, Morin E, Helman D, et al. (2020) Eco-hydrology and geomorphology of the largest floods along the hyperarid Kuiseb River, Namibia. *Journal of Hydrology* 582: 124450.
Guo Y, Huang CC, Zhou Y, et al. (2016) Extraordinary flood events and the response to monsoonal climatic change during the last 3000 years along the middle Yangtze River valley, China. *Palaeogeography, Palaeoclimatology, Palaeoecology* 462: 70–84.
Guo Y, Huang CC, Pang J, et al. (2017) Reconstruction palaeoflood hydrology using slackwater flow depth method in the Yanhe River valley, middle Yellow River basin, China. *Journal of Hydrology* 544: 156–171.
Harden TM and O'Connor JE (2017) *Prehistoric Floods on the Tennessee River—Assessing the Use of Stratigraphic Records of Past Floods for Improved Flood-Frequency Analysis. Scientific Investigations Report 2017-5052*Reston, VA: U.S. Geological Survey.
Harden T, Macklin MG, and Baker VR (2010) Holocene flood histories in south-western USA. *Earth Surface Processes and Landforms* 35: 707–716.
Harden TM, O'Connor JE, Driscoll DG, and Stamm JF (2011) *Flood-Frequency Analyses From Paleoflood Investigations for Spring, Rapid, Boxelder, and Elk Creeks, Black Hills, Western South Dakota. Scientific Investigations Report 2011-5131*. Reston, VA: U.S. Geological Survey.
Harden TM, O'Connor JE, and Driscoll DG (2015) Late Holocene flood probabilities in the Black Hills, South Dakota with emphasis on the Medieval Climate Anomaly. *Catena* 130: 62–68.

Harvey AM, Alexander RW, and James PA (1984) Lichens, soil development and the age of Holocene valley floor landforms: Howgill Fells, Cumbria. *Geografiska Annaler. Series A, Physical Geography* 66: 353–366.
Hattingh J and Zawada PK (1996) Relief peels in the study of palaeoflood slack-water sediments. *Geomorphology* 16: 121–126.
Heine K (2004) Flood reconstructions in the Namib Desert, Namibia and Little Ice Age climatic implications: Evidence from slackwater deposits and desert soil sequences. *Journal of the Geological Society of India* 64: 535–547.
Heine K and Völkel J (2011) Extreme floods around AD 1700 in the northern Namib desert, Namibia, and in the orange river catchment, South Africa—Were they forced by a decrease of solar irradiance during the little ice age? *Geographia Polonica* 84: 61–80.
Herget J (2020) Palaeostage Indicators in Rivers—An Illustrated Review. In: Herget J and Fontana A (eds.) *Palaeohydrology: Traces, Tracks and Trails of Extreme Events*, pp. 187–211. Cham: Springer International Publishing.
Hosman KJ and Ely LL (2003) Holocene paleoflood hydrology of the lower Deschutes River, Oregon. In: O'Connor JE and Grant GE (eds.) *A Peculiar River: Geology, Geomorphology, and Hydrology of the Deschutes River, Oregon*, pp. 121–146. Washington, DC: American Geophysical Union.
House PK and Baker VR (2001) Paleohydrology of flash floods in small desert watersheds in western Arizona. *Water Resources Research* 37: 1825–1839.
House PK, Pearthree PA, and Klawon JE (2002) Historical flood and paleoflood chronology of the Lower Verde River, Arizona: Stratigraphic evidence and related uncertainties. In: House PK, Webb RH, Baker VR, and Levish DR (eds.) *Ancient Floods, Modern Hazards: Principles and Applications of Paleoflood Hydrology*, pp. 267–293. Washington, DC: American Geophysical Union.
Hu G, Huang CC, Zhou Y, et al. (2016) Extreme paleoflood events 3200–3000 a BP in the Jingyuan–Jingtai reaches of the upper Yellow River, China. *Holocene* 26: 790–800.
Huang CC, Pang J, Zha X, et al. (2011) Extraordinary floods related to the climatic event at 4200 a BP on the Qishuihe River, middle reaches of the Yellow River, China. *Quaternary Science Reviews* 30: 460–468.
Huang CC, Pang J, Zha X, et al. (2012) Sedimentary records of extraordinary floods at the ending of the mid-Holocene climatic optimum along the Upper Weihe River, China. *Holocene* 22: 675–686.
Huang CC, Pang J, Zha X, et al. (2013) Extraordinary hydro-climatic events during the period AD 200–300 recorded by slackwater deposits in the upper Hanjiang River valley, China. *Palaeogeography Palaeoclimatology Palaeoecology* 374: 274–283.
Hydrologic Engineering Center (2010) *HEC-RAS, River Analysis System, Hydraulics Version 4.1*. Davis, CA: U.S. Army Corps of Engineers.
Innes JL (1985) Lichenometry. *Progress in Physical Geography: Earth and Environment* 9: 187–254.
Jacobson R, O'Connor JE, and Oguchi T (2016) Surficial geological tools in fluvial geomorphology. In: Kondolf MG and Piégay H (eds.) *Tools in Fluvial Geomorphology*, pp. 15–40. Chichester: Wiley.
Jacoby Y, Grodek T, Enzel Y, et al. (2008) Late Holocene upper bounds of flood magnitudes and twentieth century large floods in the ungauged, hyperarid alluvial Nahal Arava, Israel. *Geomorphology* 95: 274–294.
Jarrett RD (1984) Hydraulics of high-gradient streams. *Journal of Hydraulic Engineering* 110: 1519–1539.
Jarrett RD (1985) *Determination of Roughness Coefficients for Streams in Colorado. Water-Resources Investigations Report 85-4004.* U.S. Geological Survey.
Jarrett RD (1987) Errors in slope-area computations of peak discharges in mountain streams. *Journal of Hydrology* 96: 53–67.
Jarrett RD (1990) Hydrologic and hydraulic research in mountain rivers. *Water Resources Bulletin* 26: 419–429.
Jarrett RD and England JF (2002) Reliability of paleostage indicators for paleoflood studies. In: House PK, Webb RH, Baker VR, and Levish DR (eds.) *Ancient Floods, Modern Hazards: Principles and Applications of Paleoflood Hydrology*, pp. 91–109. Washington, DC: American Geophysical Union.
Jones AF, Macklin MG, and Brewer PA (2012) A geochemical record of flooding on the upper River Severn, UK, during the last 3750 years. *Geomorphology* 179: 89–105.
Kale VS, Mishra S, and Baker VR (1997) A 2000-year palaeoflood record from Sakarghat on Narmada, central India. *Journal of the Geological Society of India* 50: 283–288.
Kale VS, Mishra S, and Baker VR (2003) Sedimentary records of palaeofloods in the bedrock gorges of the Tapi and Narmada rivers, central India. *Current Science* 84: 1072–1079.
Kale V, Achyuthan H, Jaiswal M, and Sengupta S (2010) Palaeoflood Records from Upper Kaveri River, Southern India: Evidence for Discrete Floods During Holocene. *Geochronometria* 37: 49–55.
Kämpf L, Plessen B, Lauterbach S, et al. (2019) Stable oxygen and carbon isotopes of carbonates in lake sediments as a paleoflood proxy. *Geology* 48: 3–7.
Kidson RL, Richards KS, and Carling PA (2006) Hydraulic model calibration for extreme floods in bedrock-confined channels: Case study from northern Thailand. *Hydrological Processes* 20: 329–344.
Kim S-H and Tanaka Y (2017) Palaeoflood records of the last three centuries from the Pyeongchang and Dong rivers, South Korea. *Geomorphology* 290: 211–221.
King HW (1954) *Handbook of Hydraulics*. New York, NY: McGraw-Hill.
Knox JC (1985) Responses of floods to Holocene climatic change in the upper Mississippi Valley. *Quaternary Research* 23: 287–300.
Knox JC (2000) Sensitivity of modern and Holocene floods to climate change. *Quaternary Science Reviews* 19: 439–457.
Knox JC and Daniels JM (2002) Watershed scale and the stratigraphic record of large floods. In: House PK, Webb RH, Baker VR, and Levish DR (eds.) *Ancient Floods, Modern Hazards*, pp. 237–255. Washington, DC: American Geophysical Union.
Kochel RC and Baker VR (1982) Paleoflood Hydrology. *Science* 215: 353–361.
Kochel RC and Baker VR (1988) Paleoflood analysis using slackwater deposits. In: Baker RV, Kochel RC, and Patton PC (eds.) *Flood Geomorphology*, pp. 357–376. New York, NY: Wiley.
Kochel RC, Baker VR, and Patton PC (1982) Paleohydrology of southwestern Texas. *Water Resources Research* 18: 1165–1183.
Koenig TA, Bruce JL, O'Connor J, et al. (2016) *Identifying and Preserving High-Water Mark Data. Techniques and Methods 3-A24.* Reston, VA: U.S. Geological Survey.
Komar PD (1989) Flow-competence evaluations of the hydraulic parameters of floods: An assessment of the technique. In: Beven K and Carling P (eds.) *Floods: Hydrological, Sedimentological and Geomorphological Implications*, pp. 107–134. New York: Wiley.
Komar PD (1996) Entrainment of sediments from deposits of mixed grain sizes and densities. In: Carling PA and Dawson MR (eds.) *Advances in Fluvial Dynamics and Stratigraphy*, pp. 127–181. Chichester: Wiley.
Komar PD and Carling PA (1991) Grain sorting in gravel-bed streams and the choice of particle sizes for flow-competence evaluations. *Sedimentology* 38: 489–502.
Lai YG (2008) *SRH-2D Version 2: Theory and User's Manual, Sedimentation and River Hydraulics—Two-Dimensional River Flow Modeling*. Denver: Bureau of Reclamation.
Lai YG (2010) Two-dimensional depth-averaged flow modeling with an unstructured hybrid mesh. *Journal of Hydraulic Engineering* 136: 12–23.
Lam D, Croke J, Thompson C, and Sharma A (2017a) Beyond the gorge: Palaeoflood reconstruction from slackwater deposits in a range of physiographic settings in subtropical Australia. *Geomorphology* 292: 164–177.
Lam D, Thompson C, and Croke J (2017b) Improving at-site flood frequency analysis with additional spatial information: A probabilistic regional envelope curve approach. *Stochastic Environmental Research and Risk Assessment* 31: 2011–2031.
Lam D, Thompson C, Croke J, et al. (2017c) Reducing uncertainty with flood frequency analysis: The contribution of paleoflood and historical flood information. *Water Resources Research* 53: 2312–2327.
Lamb MP and Fonstad MA (2010) Rapid formation of a modern bedrock canyon by a single flood event. *Nature Geoscience* 3: 477.
Lang M, Fernandez Bono JF, Recking A, et al. (2004) Methodological guide for paleoflood and historical peak discharge estimation. In: Benito G and Thorndycraft VR (eds.) *Systematic, Palaeoflood and Historical Data for the Improvement of Flood Risk Estimation: Methodological Guidelines*, pp. 43–53. Spain: CSIC Madrid.
Lang M, Ouarda TBMJ, and Bobée B (1999) Towards operational guidelines for over-threshold modeling. *Journal of Hydrology* 225: 103–117.
Larsen IJ and Lamb MP (2016) Progressive incision of the Channeled Scablands by outburst floods. *Nature* 538: 229.
Levish DR (2002) Paleohydrologic Bounds: Nonexceedance information for flood hazard assessment. In: House PK, Webb RH, Baker VR, and Levish DR (eds.) *Ancient Floods, Modern Hazards: Principles and Applications of Paleoflood Hydrology. Water Science and Application Series*, vol. 5, pp. 175–190. Washington, DC: American Geophysical Union.

Levish DR, Ostenaa DA, and O'Connell DH (1996) Paleohydrologic bounds and the frequency of extreme floods on the Santa Ynez river, California. In: *California Weather Symposium, A Prehistoric look at California Rainfall and Floods* 1–19.
Lewin J, Ashworth PJ, and Strick RJP (2017) Spillage sedimentation on large river floodplains. *Earth Surface Processes and Landforms* 42: 290–305.
Li X and Huang CC (2017) Holocene palaeoflood events recorded by slackwater deposits along the Jin-shan Gorges of the middle Yellow River, China. *Quaternary International* 453: 85–95.
Li Y, Huang C, Ngo HH, et al. (2019) In situ reconstruction of long-term extreme flooding magnitudes and frequencies based on geological archives. *Science of the Total Environment* 670: 8–17.
Lim J, Lee J-Y, Hong S-S, and Kim J-Y (2013) Late Holocene flooding records from the floodplain deposits of the Yugu River, South Korea. *Geomorphology* 180: 109–119.
Liu T, Huang CC, Pang J, et al. (2014) Extraordinary hydro-climatic events during 1800–1600yr BP in the Jin–Shaan Gorges along the middle Yellow River, China. *Palaeogeography, Palaeoclimatology, Palaeoecology* 410: 143–152.
Liu T, Huang CC, Pang J, et al. (2015) Late Pleistocene and Holocene palaeoflood events recorded by slackwater deposits in the upper Hanjiang River valley, China. *Journal of Hydrology* 529: 499–510.
Liu T, Greenbaum N, Baker VR, et al. (2019) Paleoflood hydrology on the lower Green River, upper Colorado River Basin, USA: An example of a naturalist approach to flood-risk analysis. *Journal of Hydrology* 580: 124337.
Machado MJ, Botero BA, Lopez J, et al. (2015) Flood frequency analysis of historical flood data under stationary and non-stationary modelling. *Hydrology and Earth System Sciences* 19: 2561–2576.
Machado MJ, Medialdea A, Calle M, et al. (2017) Historical palaeohydrology and landscape resilience of a Mediterranean rambla (Castellon, NE Spain): Floods and people. *Quaternary Science Reviews* 171: 182–198.
Macklin MG and Rumsby BT (2007) Changing climate and extreme floods in the British uplands. *Transactions of the Institute of British Geographers* 32: 168–186.
Macklin MG, Rumsby BT, and Heap T (1992) Flood alluviation and entrenchment: Holocene valley-floor development and transformation in the British uplands. *Geological Society of America Bulletin* 104: 631–643.
Macklin MG, Tooth S, Brewer PA, et al. (2010) Holocene flooding and river development in a Mediterranean steepland catchment: The Anapodaris Gorge, south central Crete, Greece. *Global and Planetary Change* 70: 35–52.
Macklin MG, Lewin J, and Woodward JC (2012) The fluvial record of climate change. *Philosophical Transactions of the Royal Society A* 370: 2143–2172.
Macklin MG, Toonen WHJ, Woodward JC, et al. (2015) A new model of river dynamics, hydroclimatic change and human settlement in the Nile Valley derived from meta-analysis of the Holocene fluvial archive. *Quaternary Science Reviews* 130: 109–123.
Magilligan FJ, Goldstein PS, Fisher GB, et al. (2008) Late Quaternary hydroclimatology of a hyper-arid Andean watershed: Climate change, floods, and hydrologic responses to the El Niño-Southern Oscillation in the Atacama Desert. *Geomorphology* 101: 14–32.
Maizels JK (1983) Palaeovelocity and palaeodischarge determination for coarse gravel deposits. In: Gregory KJ (ed.) *Background to Palaeohydrology*, pp. 101–139. Chichester: Wiley.
Mandli KT, Ahmadia AJ, Berger M, et al. (2016) Clawpack: building an open source ecosystem for solving hyperbolic PDEs. *PeerJ Computer Science* 2: e68.
Manville V (2010) An overview of break-out floods from intracaldera lakes. *Global and Planetary Change* 70: 14–23.
Manville V, Hodgson KA, and Nairn IA (2007) A review of break-out floods from volcanogenic lakes in New Zealand. *New Zealand Journal of Geology and Geophysics* 50: 131–150.
Mao P, Pang J, Huang C, et al. (2016) A multi-index analysis of the extraordinary paleoflood events recorded by slackwater deposits in the Yunxi Reach of the upper Hanjiang River, China. *Catena* 145: 1–14.
McCord VA (1996) Fluvial process dendrogeomorphology: Reconstruction of flood events from the Southwestern United States using flood-scarred trees. In: Dean JS, Meko DM, and Swetnam TW (eds.) *Tree-rings, Environment and Humanity*, pp. 689–699. Tucson, AZ: Radiocarbon. Special Issue.
McKee ED (1938) Original structures in Colorado River flood deposits of Grand Canyon. *Journal of Sedimentary Research* 8: 77–83.
Medialdea A, Thomsen KJ, Murray AS, and Benito G (2014) Reliability of equivalent-dose determination and age-models in the OSL dating of historical and modern palaeoflood sediments. *Quaternary Geochronology* 22: 11–24.
Miller JR, Walsh D, and Villarroel LF (2019) Use of Paleoflood Deposits to Determine the Contribution of Anthropogenic Trace Metals to Alluvial Sediments in the Hyperarid Rio Loa Basin, Chile. *Geosciences* 9: 244.
Munoz SE, Giosan L, Therrell MD, et al. (2018) Climatic control of Mississippi River flood hazard amplified by river engineering. *Nature* 556: 95–98.
Murray AS and Wintle AG (2000) Luminescence dating of quartz using an improved single-aliquot regenerative-dose protocol. *Radiation Measurements* 32: 57–73.
O'Connell DRH, Ostenaa DA, Levish DR, and Klinger RE (2002) Bayesian flood frequency analysis with paleohydrologic bound data. *Water Resources Research* 38: 161–1614.
O'Connor JE (1993) *Hydrology, Hydraulics, and Geomorphology of the Bonneville Flood*. Special Paper 274 Boulder, CO: Geological Society of America. 83 pp.
O'Connor JE and Costa JE (1993) Geologic and hydrologic hazards in glacierized basins in North America resulting from 19th and 20th century global warming. *Natural Hazards* 8: 121–140.
O'Connor JE and Webb RH (1988) Hydraulic modeling for paleoflood analysis. In: Baker VR, Kochel RC, and Patton PC (eds.) *Flood Geomorphology*, pp. 393–402. John Wiley & Sons.
O'Connor JE, Webb RH, and Baker VR (1986) Paleohydrology of pool-and-riffle pattern development: Boulder Creek, Utah. *Geological Society of America Bulletin* 97: 410–420.
O'Connor JE, Ely LL, Wohl EE, et al. (1994) A 4500-year record of large floods on the Colorado River in the Grand-Canyon, Arizona. *Journal of Geology* 102: 1–9.
O'Connor JE, Hardison JH, and Costa JE (2001) *Debris Flows From Failures Neoglacial-Age Moraine Dams in the Three Sisters and Mount Jefferson Wilderness Areas, Oregon. Professional Paper 1606*. U.S. Geological Survey.
O'Connor JE, Clague JJ, Walder JS, et al. (2013) Outburst Floods. In: Shroder JF and Wohl E (eds.) *Treatise on Geomorphology*, pp. 475–510. San Diego, CA: Academic Press.
O'Connor JE, Atwater BF, Cohn TA, et al. (2014) *Assessing Inundation Hazards to Nuclear Powerplant Sites Using Geologically Extended Histories of Riverine Floods, Tsunamis, and Storm Surges. Scientific Investigations Report 2014–5207*. U.S. Geological Survey.
Ortega JA and Garzón G (2009) A contribution to improved flood magnitude estimation in base of palaeoflood record and climatic implications—Guadiana River (Iberian Peninsula). *Natural Hazards and Earth System Sciences* 9: 229–239.
Osterkarmp WR and Hupp CR (1984) Geomorphic and vegetative characteristics along three northern Virginia streams. *Geological Society of America Bulletin* 95: 1093–1101.
Partridge J and Baker VR (1987) Paleoflood hydrology of the Salt River, Arizona. *Earth Surface Processes and Landforms* 12: 109–125.
Patton PC, Pickup G, and Price DM (1993) Holocene paleofloods of the Ross River, Central Australia. *Quaternary Research* 40: 201–212.
Porat N (2006) Use of magnetic separation for purifying quartz for luminescence dating. *Ancient TL* 24: 33–36.
Redmond KT, Enzel Y, House PK, and Biondi F (2002) Climate variability and flood frequency at decadal to millennial time scales. In: House PK, Webb RH, Baker VR, and Levish DR (eds.) *Ancient Floods, Modern Hazards, Principles and Applications of Paleoflood Hydrology*, pp. 21–45. Washington, DC: American Geophysical Union.
Rico M, Benito G, and Barnolas A (2001) Combined palaeoflood and rainfall–runoff assessment of mountain floods (Spanish Pyrenees). *Journal of Hydrology* 245: 59–72.
Rodnight H, Duller GAT, Wintle AG, and Tooth S (2006) Assessing the reproducibility and accuracy of optical dating of fluvial deposits. *Quaternary Geochronology* 1: 109–120.
Rosenwinkel S, Korup O, Landgraf A, and Dzhumabaeva A (2015) Limits to lichenometry. *Quaternary Science Reviews* 129: 229–238.
Rubin DM, Schmidt JC, and Moore JN (1990) Origin, structure, and evolution of a reattachment bar, Colorado River, Grand Canyon, Arizona. *Journal of Sedimentary Research* 60: 982–991.
Ruiz-Villanueva V, Díez-Herrero A, Stoffel M, et al. (2010) Dendrogeomorphic analysis of Flash Floods in a small ungauged mountain catchment (Central Spain). *Geomorphology* 118: 383–392.
Ruiz-Villanueva V, Diez-Herrero A, Bodoque JM, et al. (2013) Characterisation of flash floods in small ungauged mountain basins of Central Spain using an integrated approach. *Catena* 110: 32–43.

Sandercock P and Wyrwoll KH (2005) The historical and palaeoflood record of Katherine river, northern Australia: Evaluating the likelihood of extreme discharge events in the context of the 1998 flood. *Hydrological Processes* 19: 4107–4120.
Schillereff DN, Chiverrell RC, Macdonald N, and Hooke JM (2016) Hydrological thresholds and basin control over paleoflood records in lakes. *Geology* 44: 43–46.
Schmidt JC (1990) Recirculating flow and sedimentation in the Colorado River in Grand Canyon, Arizona. *The Journal of Geology* 98: 709–724.
Schneuwly-Bollschweiler M, Corona C, and Stoffel M (2013) How to improve dating quality and reduce noise in tree-ring based debris-flow reconstructions. *Quaternary Geochronology* 18: 110–118.
Schulte L, Peña JC, Carvalho F, et al. (2015) A 2600-year history of floods in the Bernese Alps, Switzerland: Frequencies, mechanisms and climate forcing. *Hydrology and Earth System Sciences* 19: 3047–3072.
Schulte L, Wetter O, Wilhelm B, et al. (2019) Integration of multi-archive datasets for the development of a four-dimensional paleoflood model of alpine catchments. *Global and Planetary Change* 180: 66–88.
Sheffer NA, Enzel Y, Benito G, et al. (2003) Paleofloods and historical floods of the Ardeche River, France. *Water Resources Research* 39: 1376.
Sheffer NA, Rico M, Enzel Y, et al. (2008) The Palaeoflood record of the Gardon River, France: A comparison with the extreme 2002 flood event. *Geomorphology* 98: 71–83.
Sigafoos RS (1964) *Botanical Evidence of Floods and Flood-Plain Deposition. Professional Paper 485*. U.S. Geological Survey.
Smedley RK and Skirrow GKA (2020) Luminescence dating in fluvial settings: Overcoming the challenge of partial bleaching. In: Herget J and Fontana A (eds.) *Palaeohydrology: Traces, Tracks and Trails of Extreme Events*, pp. 155–168. Cham: Springer International Publishing.
Smith AM (1992) Palaeoflood Hydrology of the Lower Umgeni River from a Reach South of the Inanda Dam, Natal. *South African Geographical Journal* 74: 63–68.
Solomina ON, Savoskul OS, and Cherkinsky AE (1994) Glacier variations, mudflow activity and landscape development in the Aksay Valley (Tian Shan) during the late Holocene. *The Holocene* 4: 25–31.
Springer GS and Kite JS (1997) River-derived slackwater sediments in caves along Cheat River, West Virginia. *Geomorphology* 18: 91–100.
Sridhar A (2007) A mid–late Holocene flood record from the alluvial reach of the Mahi River, Western India. *Catena* 70: 330–339.
Sridhar A, Chamyal LS, and Patel M (2014) Palaeoflood record of high-magnitude events during historical time in the Sabarmati River, Gujarat. *Current Science* 107: 675–679.
St George S (2010) Tree rings as paleoflood and paleostage indicators. In: Stoffel M, Bollschweiler M, Butler DR, and Luckman BH (eds.) *Tree Rings and Natural Hazards: A State-of-the-Art*, pp. 233–239. Advances in Global Change Research.
St George S and Nielsen E (2003) Palaeoflood records for the Red River, Manitoba, Canada, derived from anatomical tree-ring signatures. *The Holocene* 13: 547–555.
St George S, Erik N, France C, and Tardif J (2002) Trends in Quercus macrocarpa vessel areas and their implications for tree-ring paleoflood studies. *Tree-Ring Research* 58: 3–10.
Stedinger JR and Baker VR (1987) Surface water hydrology: Historical and paleoflood information. *Reviews of Geophysics* 25: 119–124.
Stedinger JR and Cohn TA (1986) Flood frequency analysis with historical and paleoflood information. *Water Resources Research* 22: 785–793.
Stokes S and Walling DE (2003) Radiogenic and isotopic methods for the direct dating of fluvial sediments. In: Kondolf GM and Piégay H (eds.) *Tools in Fluvial Geomorphology*, pp. 233–267. Chichester: J. Wiley and Sons.
Swain RE, England Jr, JF, Bullard KL, and Raff DA (2004) Hydrologic hazard curve estimating procedures. *Bureau of Reclamation Research Report DSO-04-08*. pp. 79.
Sweeney KE and Roering JJ (2017) Rapid fluvial incision of a late Holocene lava flow: Insights from LiDAR, alluvial stratigraphy, and numerical modeling. *GSA Bulletin* 129: 500–512.
Therrell MD and Bialecki MB (2015) A multi-century tree-ring record of spring flooding on the Mississippi River. *Journal of Hydrology* 529: 490–498.
Thorndycraft VR, Benito G, Rico M, et al. (2005a) A long-term flood discharge record derived from slackwater flood deposits of the Llobregat River, NE Spain. *Journal of Hydrology* 313: 16–31.
Thorndycraft VR, Benito G, Walling DE, et al. (2005b) Caesium-137 dating applied to slackwater flood deposits of the Llobregat River, NE Spain. *Catena* 59: 305–318.
Toonen WHJ (2015) Flood frequency analysis and discussion of non-stationarity of the Lower Rhine flooding regime (AD 1350–2011): Using discharge data, water level measurements, and historical records. *Journal of Hydrology* 528: 490–502.
Toonen WHJ, Kleinhans MG, and Cohen KM (2012) Sedimentary architecture of abandoned channel fills. *Earth Surface Processes and Landforms* 37: 459–472.
Toonen WHJ, Winkels TG, Cohen KM, et al. (2015) Lower Rhine historical flood magnitudes of the last 450years reproduced from grain-size measurements of flood deposits using End Member Modelling. *Catena* 130: 69–81.
Toonen WHJ, Munoz SE, Cohen KM, and Macklin MG (2020) High-Resolution Sedimentary Paleoflood Records in Alluvial River Environments: A Review of Recent Methodological Advances and Application to Flood Hazard Assessment. In: Herget J and Fontana A (eds.) *Palaeohydrology: Traces, Tracks and Trails of Extreme Events*, pp. 213–228. Cham: Springer International Publishing.
Trumbore S (2000) Age of soil organic matter and soil respiration: Radiocarbon constraints on belowground c dynamics. *Ecological Applications* 10: 399–411.
Turzewski MD, Huntington KW, and LeVeque RJ (2019) The Geomorphic Impact of Outburst Floods: Integrating Observations and Numerical Simulations of the 2000 Yigong Flood, Eastern Himalaya. *Journal of Geophysical Research - Earth Surface* 124: 1056–1079.
Veilleux AG, Cohn TA, Flynn KM, et al. (2014) *Estimating magnitude and frequency of floods using the PeakFQ 7.0 program. Fact Sheet 2013–3108*. Reston, VA: U.S. Geological Survey.
Wan H, Huang C, Ge B, and Pang J (2019) Hydrological reconstruction of Holocene Paleofloods in Baoji—Tianshui gorge, upper Weihe River basin, China. *Quaternary International* 521: 138–146.
Wang L and Leigh DS (2012) Late-Holocene paleofloods in the Upper Little Tennessee River valley, Southern Blue Ridge Mountains, USA. *The Holocene* 22: 1061–1066.
Wang M, Zheng H, Xie X, et al. (2011) A 600-year flood history in the Yangtze River drainage: Comparison between a subaqueous delta and historical records. *Chinese Science Bulletin* 56: 188–195.
Wasson RJ, Sundriyal YP, Chaudhary S, et al. (2013) A 1000-year history of large floods in the Upper Ganga catchment, central Himalaya, India. *Quaternary Science Reviews* 77: 156–166.
Waythomas CF and Jarrett RD (1994) Flood geomorphology of Arthurs Rock Gulch, Colorado: Paleoflood history. *Geomorphology* 11: 15–40.
Webb RH and Jarrett RD (2002) One-dimensional estimation techniques for discharges of paleofloods and historical floods. In: House PK, Webb RH, Baker VR, and Levish DR (eds.) *Ancient Floods, Modern Hazards: Principles and Applications of Paleoflood Hydrology*, pp. 111–125. Washington, DC: American Geophysical Union.
Webb RH, O'Connor JE, and Baker VR (1988) Paleohydrologic reconstruction of flood frequency on the Escalante River, South-central Utah. In: *Flood Geomorphology*. New York: John Wiley & Sons.
Webb RH, Blainey JB, and Hyndman DW (2002) Paleoflood hydrology of the Paria River, Southern Utah and northern Arizona, USA. In: House PK, Webb RH, Baker VR, and Levish DR (eds.) *Ancient Floods, Modern Hazards: Principles and Applications of Paleoflood Hydrology*, pp. 295–310. Washington, DC: American Geophysical Union.
Wells LE (1990) Holocene history of the El Niño phenomenon as recorded in flood sediments of northern coastal Peru. *Geology* 18: 1134–1137.
Wertz EL, St. George S, and Zeleznik JD (2013) Vessel anomalies in Quercus macrocarpa tree rings associated with recent floods along the Red River of the North, United States. *Water Resources Research* 49: 630–634.
Wilcock PR, Billi P, Hey RD, and Thorne CR (1992) Bed-load transport of mixed-size sediment. In: Tacconi P (ed.) *Dynamics of Gravel-Bed Streams*, pp. 109–131. Chichester: Wiley.
Wild E, Golser R, Hille P, et al. (1997) First 14C Results from Archaeological and Forensic Studies at the Vienna Environmental Research Accelerator. *Radiocarbon* 40: 273–281.
Wilhelm B, Arnaud F, Sabatier P, et al. (2012) 1400 years of extreme precipitation patterns over the Mediterranean French Alps and possible forcing mechanisms. *Quaternary Research* 78: 1–12.
Wilhelm B, Vogel H, Crouzet C, et al. (2016) Frequency and intensity of palaeofloods at the interface of Atlantic and Mediterranean climate domains. *Climate of the Past* 12: 299–316.
Wilhelm B, Ballesteros Canovas JA, Corella Aznar JP, et al. (2018) Recent advances in paleoflood hydrology: From new archives to data compilation and analysis. *Water Security* 3: 1–8.

Wilhelm B, Ballesteros Cánovas JA, Macdonald N, et al. (2019) Interpreting historical, botanical, and geological evidence to aid preparations for future floods. *Wiley Interdisciplinary Reviews Water* 6: e1318.
Williams GP (1983) Paleohydrological methods and some examples from Swedish fluvial environments: I. Cobble and boulder deposits. *Geografiska Annaler* 65: 227–243.
Williams GP (1984) Paleohydrologic equations for rivers. In: Costa JE and Fleisher PJ (eds.) *Developments and Applications of Geomorphology*, pp. 343–367. Berlin: Springer-Verlag.
Williams GP and Costa JE (1988) Geomorphic measurements after a flood. In: Baker RV, Kochel RC, and Patton PC (eds.) *Flood Geomorphology*, pp. 65–77. New York: John Wiley & Sons.
Wintle AG and Murray AS (2006) A review of quartz optically stimulated luminescence characteristics and their relevance in single-aliquot regeneration dating protocols. *Radiation Measurements* 41: 369–391.
Wirth S, Glur L, Gilli A, and Anselmetti F (2013) Holocene flood frequency across the Central Alps—Solar forcing and evidence for variations in North Atlantic atmospheric circulation. *Quaternary Science Reviews* 80: 112–128.
Wohl EE (1992) Bedrock benches and boulder bars—Floods in the Burdekin Gorge of Australia. *Geological Society of America Bulletin* 104: 770–778.
Wohl EE, Fuertsch SJ, and Baker VR (1994) Sedimentary records of Late Holocene floods along the Fitzroy and Margaret rivers, Western-Australia. *Australian Journal of Earth Sciences* 41: 273–280.
Yang DY, Yu G, Xie YB, et al. (2000) Sedimentary records of large Holocene floods from the middle reaches of the Yellow River, China. *Geomorphology* 33: 73–88.
Yanosky TM (1984) Documentation of high summer flows on the Potomac River from the wood anatomy of ash trees. *JAWRA Journal of the American Water Resources Association* 20: 241–250.
Yu SY, Zhu C, and Wang F (2003) Radiocarbon constraint on the Holocene flood deposits of the Ning-Zhen Mountains, lower Yangtze River area of China. *Journal of Quaternary Science* 18: 521–525.
Zawada PK (1994) Palaeoflood hydrology of the Buffels River, Laingsburg, South Africa: Was the 1981 flood the largest? *South African Journal of Geology* 97: 21–32.
Zawada PK (2000) Slackwater sediments and paleofloods. Their significance for Holocene paleoclimatic reconstruction and flood prediction. In: Partridge TC and Maud RR (eds.) *Cenozoic of Southern Africa*, pp. 198–206. New York: Oxford University Press.
Zhan W, Yang S, Liu X, et al. (2010) Reconstruction of flood events over the last 150 years in the lower reaches of the Changjiang River. *Chinese Science Bulletin* 55: 2268–2274.
Zhang Y, Huang CC, Pang J, et al. (2012) Comparative study of the modern flood slackwater deposits in the upper reaches of Hanjiang and Weihe River Valleys, China. *Quaternary International* 282: 184–191.
Zhang Y, Huang CC, Pang J, et al. (2013) Holocene paleofloods related to climatic events in the upper reaches of the Hanjiang River valley, middle Yangtze River basin, China. *Geomorphology* 195: 1–12.
Zhou L, Huang CC, Zhou Y, et al. (2016) Late Pleistocene and Holocene extreme hydrological event records from slackwater flood deposits of the Ankang east reach in the upper Hanjiang River valley, China. *Boreas* 45: 673–687.
Zhu C, Zheng C, Ma C, et al. (2005) Identifying paleoflood deposits archived in Zhongba Site, the Three Gorges reservoir region of the Yangtze River, China. *Chinese Science Bulletin* 50: 2493–2504.